AD 652697

essa Technical Report

INSTITUTES FOR ENVIRONMENTAL RESEARCH   IER 37-ITSA 37

Application of Statistical Estimation Techniques to Ground-Based Passive Probing of the Tropospheric Temperature Structure
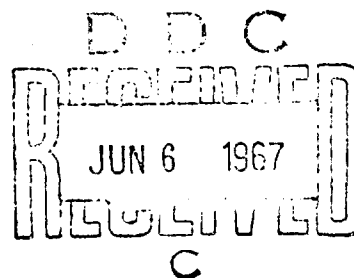
ED R. WESTWATER

OTTO NEALL STRAND

Sponsored by:

ECOM

D D C

JUN 6 1967

C

UNITED STATES ARMY ELECTRONICS COMMAND · FORT MONMOUTH, N.J.

APRIL, 1967

ARCHIVE COPY

Boulder, Colorado

92

THE INSTITUTES FOR ENVIRONMENTAL RESEARCH

The mission of the Institutes is to study the oceans, and inland waters, the lower and upper atmosphere, the space environment, and the earth, seeking the understanding needed to provide more useful services. These research Institutes are:

- The Institute for Earth Sciences
    conducts exploratory and applied research in geomagnetism, seismology, geodesy, and related earth sciences.

- The Institute for Oceanography
    works to increase knowledge and improve understanding of the ocean and its interaction with the total physical environment of the globe.

- The Institute for Atmospheric Sciences
    seeks the understanding of atmospheric processes and phenomena that is required to improve weather forecasts and related services and to modify and control the weather.

- The Institute for Telecommunication Sciences and Aeronomy
    supports the Nation's telecommunications by conducting research and providing services related to radio, infrared, and optical waves as they travel from a transmitter to a receiver. The Institute is also active in the study and prediction of periods of solar activity and ionospheric disturbance.

Environmental Science Services Administration
Boulder, Colo.

ESSA TECHNICAL REPORT   IER 37-ITSA 37

Application of Statistical Estimation Techniques to Ground-Based Passive Probing of the Tropospheric Temperature Structure

ED R. WESTWATER

OTTO NEALL STRAND

NOTICES

Disclaimers

The findings in this report are not to be construed as an official Department of the Army position, unless so designated by other authorized documents.

The citation of trade names and names of manufacturers in this report is not to be construed as official Government indorsement or approval of commercial products or services referenced herein.

Disposition

Destroy this report when it is no longer needed. Do not return it to the originator.

This Final Report has been prepared for the U.S. Army Electronics Command, Fort Monmouth, New Jersey, as a partial fulfillment of the requirements of MIPR NO. R66-7-AMC-00-91.

Table of Contents

iii

APPLICATION OF STATISTICAL ESTIMATION TECHNIQUES TO GROUND-BASED PASSIVE PROBING OF THE TROPOSPHERIC TEMPERATURE STRUCTURE

by

Ed R. Westwater

and

Otto Neall Strand

Abstract

The theory of radiative transfer in the microwave region is discussed. A method for the numerical solution of a Fredholm integral equation of the first kind is derived and illustrated. The method employs an a priori constraint vector together with covariances of both the constraint vector and the measurement errors. The method automatically incorporates an optimum amount of smoothing in the sense of maximum-likelihood estimation. The problem of obtaining optimum basis vectors is discussed. The trace of the covariance matrix of the error in the solution is used to estimate the accuracy of the results. This trace is used to derive a quality criterion for a set of measurements and a given set of constraint statistics. Examples are given in which the behavior of the solution as obtained from a specific integral equation is studied by the use of random input errors to simulate measurement errors and statistical sampling. The quality criterion and behavior of the trace of the error covariance matrix for various bases are also illustrated for the equation being considered. A least-squares analysis of microwave absorption data to determine line width for water vapor and oxygen is presented. Calculations of the error covariance matrix and quality-criterion values to be expected when probing for the tropospheric temperature structure from microwave emission measurements are presented.

1. Introduction

The general subject of passive probing of the atmosphere by electromagnetic means has recently received attention by several authors: Fleming and Wark, [1]; Kaplan [2]; and King, [3]. In spite of the wide differences in the specific techniques applied to each spectral region, several elements are common to all passive probing schemes. The first of these elements is the sensor, which measures relevant properties of the radiation emanating from the spatial region being probed. Secondly, detailed knowledge is required concerning the mechanisms by which radiation is generated at the region being probed and by which the radiation is propagated to the sensor. The last, but certainly not the least, is the manner by which information concerning the physical property of interest is derived from the set of radiation measurements, the so-called "inversion process".

The probing methods discussed here attempt to derive information about the temperature distribution of the troposphere by measuring the microwave brightness temperature of the atmosphere from the ground looking up. The propagation and emission of this radiation are determined for the most part by the absorption coefficients of oxygen and water vapor.

The inversion method we derive here is illustrated for the physical situation of ground-based upward probing; however, the inversion equations are applicable to more general situations. This technique extends methods given by Phillips [4], Twomey [5],[6], and Twomey and Howell [7] for the solution of integral equations of the first kind. These methods use a controlled amount of smoothing in solving the matrix system derived from a quadrature approximation, but give no systematic method of determining the required amount of smoothing. In this paper, we derive and illustrate a general least-squares process for estimating the solution and show that it contains Twomey's method of weighting an a priori constraint vector as a special case. The optimum amount of smoothing (in the sense of maximum-likelihood estimation) depends on certain covariance matrices describing the measurement process. In a manner similar to that of the more recent work [8], [9], [10], and [11], we derive and use statistically orthogonal basis vectors.

Certain other bases are also used and numerical comparisons are made for a particular kernel. In our method, the covariance matrix of the error in the resulting solution is calculated and its trace is used as a measure of the error in the final results. It is shown in this paper that the trace of the error covariance matrix is minimized when the number of basis vectors equals the number of quadrature points. We use the resulting minimum trace as a quality criterion describing the effectiveness of a given matrix equation (with specified accuracy of observation and a specified distribution of the constraint vector) in reducing the variance of the a priori constraint vector. We also derive and discuss the condition for an optimum basis and present numerical examples using random input errors to simulate the measurement process. We discuss and present a least-squares analysis of line width and absorption data for both water vapor and oxygen. We also present numerous calculations of the solution quality criterion and indicate how this criterion could be used to determine both experimental feasibility and optimum choice of probing frequencies.

2. Theory of Radiative Transfer in the Microwave Region

The equation of transfer in a steady field of radiation in the case of local thermodynamic equilibrium is given by Kondrat'yev [12]

4

$$\frac{\cos \theta}{\rho} \frac{\partial I_\nu}{\partial h} = \kappa_\nu B_\nu + \frac{\sigma_\nu}{4\pi} \int I_\nu(h, r') p_\nu(h, r', r)\, d\omega' - (\kappa_\nu + \sigma_\nu) I_\nu, \qquad (1)$$

where I_ν is the intensity of radiation, θ is the zenith angle, h is the height above the surface, κ_ν and σ_ν are the mass absorption and mass scattering coefficients respectively, ρ is the density of material absorbing the radiation, B_ν is the Planck intensity function, and $\frac{d\omega'}{4\pi} p_\nu(h, r', r)$ is the fraction of energy incident upon the scattering volume in the direction r' which is scattered in the direction r.

The integration over $d\omega'$ extends over all directions of r'. For a cloudless atmosphere and for microwave frequencies, the scattering coefficient is zero and the equation of transfer for a purely absorbing atmosphere is obtained

$$\frac{\cos \theta}{\rho} \frac{\partial I_\nu}{\partial h} = \kappa_\nu (B_\nu - I_\nu) . \qquad (2)$$

This can be integrated to give

$$I_\nu(h) = I_\nu(\infty)\, e^{-\tau_\nu(h, \infty)/\cos \theta} + \int_h^\infty \kappa_\nu \rho B_\nu\, e^{-\int_h^{h'} \kappa_\nu \rho \frac{dh''}{\cos \theta}} \frac{dh'}{\cos \theta}, \qquad (3)$$

for the intensity received "looking up" at a height h and at a zenith angle θ. In (3), $I_\nu(\infty)$ is the unattenuated intensity incident outside the atmosphere and $\tau_\nu(h, \infty)$ is the total vertical attenuation given by

5

$$\tau_\nu(h, \infty) = \int_h^\infty \kappa_\nu \rho \, dh' \quad . \tag{4}$$

The Planck function, B_ν, multiplied by the absorption coefficient is proportional to the power flux density emitted per unit bandwidth and may be approximated by the Rayleigh-Jeans law in the microwave region [13]:

$$B_\nu = \frac{2\nu^2}{c^2} k \, T, \tag{5}$$

where k is the Boltzman constant, c is the speed of light, and T is the absolute temperature. The intensity, I_ν, may be related to the brightness temperature, T_{b_ν}, by the defining relation

$$I_\nu \equiv \frac{2\nu^2}{c^2} k \, T_{b_\nu} . \tag{6}$$

It follows immediately from (3), (5), and (6) that

$$T_{b_\nu}(h) = T_{b_\nu}(\infty) \, e^{-\tau_\nu(h, \infty)/\cos\theta} + \int_h^\infty \kappa_\nu \rho T \, e^{-\int_h^{h'} \kappa_\nu \rho \, dh''/\cos\theta} \frac{dh'}{\cos\theta} . \tag{7}$$

The apparent sky temperature, as measured by an antenna immersed in a radiation field, will be the contribution of (7) from

each direction seen by the antenna multiplied by the appropriate antenna gain factors and integrated over the antenna pattern.

If it is desired to determine the brightness temperature of the atmosphere from directions confined to a narrow solid angle, it is necessary to have a highly directional antenna with low side lobes such that the contributions from the desired direction are maximized. The noise temperature of the antenna can be measured directly by comparing the received signal with that of a known source.

In using (7) to deduce $T(h)$ from measurements of T_b, one may vary either zenith angle, θ, or frequency, ν. In ground-based probing, however, there are reasons to avoid the angular scheme. First, an assumption of horizontal homogeneity of the atmosphere is necessary. It is also probable that some of the space swept out by the observing antenna will include discrete cloud structures whose emission is not easily taken into account. Finally, it is very difficult to take account of ground emissions and reflections because of uncertainties in antenna gain patterns. We will therefore only consider inversion using measurements at different frequencies. This scheme reduces, but does not eliminate, the above difficulties. Henceforth, it will be assumed that no clouds are present in the main beam of the observing antenna.

Equation (7) is non-linear in the temperature because the absorption coefficient depends on temperature and pressure. As discussed by Westwater [14], this non-linearity can be handled by assuming a mean temperature profile to determine a first approximation to the absorption, solving the resulting Fredholm equation of the first kind, and iterating. The next section presents a method of solving the linearized equation in the presence of measurement error by statistically weighting a priori knowledge of the temperature profile against information given by the integral equation. Because of the nature of the constraint, it is presumed that convergence of the iteration sequence will cause no problem, even in the presence of large experimental errors. This has not yet been verified.

3. Inversion Method

Let $\{f(y), a \leq y \leq b\}$ be a Gaussian random process having continuous sample functions. If $K(x, y)$ is a continuous function of x and y and if

$$\int_a^b K(x, y) \, f(y) \, dy = g(x) \tag{8}$$

then $g(x)$ is also a Gaussian process with continuous sample functions. The main idea is to estimate $f(y)$ by measuring $g(x)$ at various values of x, say $x = x_i$, $i = 1, \ldots n$. Introducing a quadrature formula of the type $\int_a^b h(y)dy = \sum_{j=1}^m w_j h(y_j)$ gives a matrix equation

$$Af = g \qquad\qquad (9)$$

where

$A = (A_{ij})$ $i = 1, 2, \ldots n$; $j = 1, 2, \ldots m$,

m is the number of quadrature abscissas,

n is the number of observations of $g(x)$,

y_j are the quadrature abscissas,

x_i are the specific values of x for which $g(x)$ is observed,

w_j are the weights associated with y_j,

$f_j = f(y_j)$,

$g_i = g(x_i)$,

$A_{ij} = w_j K(x_i, y_j)$,

$f = [f_1 f_2 \ldots f_m]^T$ is the column vector of unknown functional values,

(the superscript T denotes matrix transposition throughout this paper),

and $g = [g_1 g_2 \ldots g_n]^T$ is the column vector of values of $g(x)$.

We assume that the mean vector $E(f) = f_o$ and the covariance matrix, S_f, of f are known. ($E(\ )$ denotes the expected-value operator and S_v denotes the covariance matrix of any vector v throughout this paper).

By the linearity of E and the propagation rule for covariance matrices, respectively, we have $E(g) = g_o = Af_o$ and $S_g = AS_f A^T$. In the cases

9

of interest here g is a vector of measurements subject to error.
Thus one observes

$$g_e = g + \varepsilon \qquad (10)$$

instead of g. In addition to the assumptions already made, we assume:

a)   the errors ε_i are independent of f, hence independent of g;

b)   the errors ε_i are normally distributed with zero mean and known covariance matrix S_ε;

c)   the quadrature errors are negligible with respect to ε;

d) S_ε and S_f are both nonsingular with dimensions $n \times n$ and $m \times m$, respectively.

It is convenient in practice to represent the solution in terms of a small number of basis vectors. We let $U = [\, U_1 \,|\, U_2 \,|\ldots|\, U_k \,]$ (lines denote matrix partitions throughout this paper) be a matrix of k linearly independent m-component basis column vectors and $C = [\, C_1 C_2 \ldots C_k \,]^T$ be a vector of coefficients to be determined where $k \leq m$.

The inference problem to be solved is the following. Given the observed vector g_e and the covariance matrices S_f and S_ε, estimate f and ε under the constraint $g_e - Af = \varepsilon$. Putting

$$\eta = f - f_0, \quad h = g - g_0 = A(f - f_0) = A\eta$$

$$h_e = h + \varepsilon = A\eta + \varepsilon, \qquad (11)$$

where η is to be approximated by UC gives an equivalent problem: given h_e, estimate η and ϵ in the form $\left[\frac{UC}{\hat{\epsilon}}\right]$ subject to the constraint $h_e - AUC = \hat{\epsilon}$. First, note that the maximum-likelihood estimate of η in the absence of measurements g_e is $\eta = 0$. The estimate $\eta = 0$ may be coupled with the set of measurements, g_e, to form an "effective" measurement vector $\left[\frac{0}{h_e}\right]$. From this vector and the Gauss-Markov least-squares principle for correlated variables [15], a maximum-likelihood estimate of $\left[\frac{\eta}{\epsilon}\right]$ can be obtained. Since the covariance matrix of $\left[\frac{\eta}{\epsilon}\right]$ is $\left[\begin{array}{c|c} S_f & 0 \\ \hline 0 & S_\epsilon \end{array}\right]$, the desired estimate $\left[\frac{UC}{\hat{\epsilon}}\right]$ must be such that $R(C, \epsilon)$ is rendered stationary, where

$$R(C, \epsilon) \equiv (UC)^T S_f^{-1} (UC) + \epsilon^T S_\epsilon^{-1} \epsilon + \mu^T (AUC - h_e + \epsilon), \qquad (12)$$

and μ^T is a row matrix of Lagrange multipliers. Differentiating with respect to C, ϵ, and μ and equating to zero gives the solution

$$UC = UD^{-1} U^T A^\perp S_\epsilon^{-1} h_e \qquad (13)$$

and

$$\hat{\epsilon} = h_e - AUD^{-1} U^T A^T S_\epsilon^{-1} h_e \quad , \qquad (14)$$

where

$$D = U^T X U \text{ and } X = S_f^{-1} + A^T S_\epsilon^{-1} A. \qquad (15)$$

11

We may also rewrite (13) in the equivalent form

$$UC = U(U^T S_f^{-1} U)^{-1} U^T A^T \left[S_\varepsilon + AU(U^T S_f^{-1} U)^{-1} U^T A^T \right]^{-1} h_e. \quad (16)$$

We apply the propagation rule for covariance matrices to $UC - \eta$, where UC is given by (13):

$$UC - \eta = UD^{-1} U^T A^T S_\varepsilon^{-1} (A\eta + \varepsilon) - \eta$$

and

$$S_{UC - \eta} = \left[UD^{-1} U^T A^T S_\varepsilon^{-1} A - I \right] S_f \left[UD^{-1} U^T A^T S_\varepsilon^{-1} A - I \right]^T$$

$$+ \left[UD^{-1} U^T A^T S_\varepsilon^{-1} \right] S_s \left[UD^{-1} U^T A^T S_\varepsilon^{-1} \right]^T,$$

so that

$$S_{UC - \eta} = TYS_f YT - (TYS_f + S_f YT) + S_f + TYT, \quad (17)$$

where

$$Y = A^T S_\varepsilon^{-1} A \text{ and } T = UD^{-1} U^T. \quad (18)$$

Substituting $Y = X - S_f^{-1}$ into (17) and noting that $TXT = T$ gives

$$S_{UC - \eta} = S_f + T + T (XS_f X) T - TXS_f - S_f XT, \quad (19)$$

and

$$S_{\hat{\varepsilon} - \varepsilon} = AS_{UC - \eta} A^T. \quad (20)$$

Expressions (13), or (16), and (14) give the desired statistical estimates of the solution for any given basis U. Equations (19) and (20) give the error covariance matrices by which the quality of the results may be estimated, as will be seen in the next section. In the work reported in this paper no use has been made of the estimate (14) of $\hat{\epsilon}$ of the expression (20) giving $S_{\hat{\epsilon} - \epsilon}$.

Various special cases may be noted. If $k = m$, that is, if U is a nonsingular $m \times m$ matrix, (13), (16), (19), and (20) become, respectively,

$$UC \equiv \hat{\eta} = X^{-1} A^T S_{\epsilon}^{-1} h_e \ , \tag{21}$$

$$\hat{\eta} = S_f A^T H^{-1} h_e \ , \tag{22}$$

$$S_{\hat{\eta} - \eta} = X^{-1} \ , \tag{23}$$

$$S_{\hat{\epsilon} - \epsilon} = AX^{-1} A^T \ , \tag{24}$$

where

$$H = S_{\epsilon} + AS_f A^T \ .$$

From (22), a result equivalent to (23) is

$$X^{-1} = S_{\hat{\eta} - \eta} = S_f P S_f P S_f - 2S_f P S_f + S_f + S_f A^T H^{-1} S_{\epsilon} H^{-1} A S_f \ , \tag{25}$$

where

$$P = A^T H^{-1} A.$$

13

The study of special cases will be confined to the case $k = m$ here. If $S_\epsilon^{-1} \to 0$, i.e., if the measurements have large errors, we obtain $\hat{\eta} = 0$ or $f = f_o$ and $S_{\hat{\eta} - \eta} = S_f$. If $S_f^{-1} \to 0$, then X will be nonsingular if and only if rank $A = m$. Then $\hat{\eta} = (A^T S_\epsilon^{-1} A)^{-1} A^T S_\epsilon^{-1} h_e$ and $S_{\hat{\eta} - \eta} = (A^T S_\epsilon^{-1} A)^{-1}$. If $S_\epsilon \to 0$, i.e., if the measurements of g are perfect, and if rank $AU = n$ then $n \leq m$ and (22) and (23) become respectively, $\hat{\eta} = S_f A^T \left[A S_f A^T \right]^{-1} h$ and $S_{\hat{\eta} - \eta} = S_f - S_f A^T (A S_f A^T)^{-1} A S_f$. In computational practice the latter situation will not occur since the quadrature errors will invalidate the assumptions as $S_\epsilon \to 0$. Finally, if $S_f \to 0$, then (22) and (25) give, respectively, $\hat{\eta} = 0$ or $f = f_o$ and $S_{\hat{\eta} - \eta} = 0$.

We may show the correspondence of the present method with that of Twomey [6] as follows: for $k = m$, let $S_\epsilon = \sigma_\epsilon^2 I$, $S_f = \sigma_f^2 I$, $\gamma = \sigma_\epsilon^2 / \sigma_f^2$, $f_o = \bar{p}$, $f_o + \hat{\eta} = \bar{f}$, and $g_e = \bar{g}$ in (21) to correspond with Twomey's notation [6]. Then

$$\bar{f} = \left[A^T A + \gamma I \right]^{-1} \left[A^T \bar{g} + \gamma \bar{p} \right], \qquad (26)$$

which is identical to Twomey's equation (6), p. 105. Thus, if the covariance matrices S_f and S_ϵ are both scalar, the optimum choice of γ (in the sense of maximum-likelihood estimation) is given by the ratio of variances. However, in commonly occuring physical situations S_f has substantial off-diagonal elements.

14

The basis $U = I$ with $m = k$ gives an adequate solution via (21), (23), and (24). However, it is often convenient to represent the solution in terms of k parameters, where $k < m$, using (13), (19), and (20). The quality of such a representation depends on the choice of basis. In the next section we discuss the problem of basis optimization.

4. Determination of Optimum Basis Vectors

Previous solutions by Wark and Fleming [10], and Twomey [11] have employed basis vectors (i.e., columns of U) which were obtained to fit the data in an optimum manner without reference to the integral equation to be solved. It will be shown below that the integral equation (as represented by the matrix A which is an ingredient of $S_{UC - \eta}$) plays a part in obtaining the optimum matrix U, but (see section 5) the use of an exactly optimum basis U is often not critical, so that U as employed in earlier solutions should suffice. This classical determination of U (as exemplified by Obukhov's paper [16], for example) is presented here and interpreted in terms of the covariance matrix of the residuals. The criterion which must be satisfied for an optimum basis for the integral equation is then easily seen.

Consider the quadratic form

$$(d - UC)^T (d - UC) \equiv q (U, C). \tag{27}$$

15

Here U and C have the same meaning as in section 3 and d is a sample vector from a population having a multivariate m-dimensional normal distribution, say, with zero mean and covariance matrix S_d. For any specified basis U, $q(U, C)$ is minimized when

$$UC = U(U^T U)^{-1} U^T d, \tag{28}$$

as can be seen by differentiation. Thus the minimum value of $q(U, C)$ for any given basis U is given by

$$q_{min.}(U) = d^T \left[U(U^T U)^{-1} U^T - I \right]^T \left[U(U^T U)^{-1} U^T - I \right] d . \tag{29}$$

Various criteria may be used to determine what is meant by "smallness" of q In the classical case the optimum U is that which minimizes the expected value of $q_{min}(U)$. Let $TrB \equiv$ trace B denote the sum of the diagonal elements of any matrix B. By expanding and employing the linearity of the operator E we may show that

$$E[d^T Q d] = Tr\, S_d\, Q \tag{30}$$

for any real symmetric matrix Q. Applying (30) to (29) gives U as that basis which minimizes

$$Tr\{ S_d [I - U(U^T U)^{-1} U^T] \}$$

$$= Tr S_d - Tr\, U^T S_d U(U^T U)^{-1} . \tag{31}$$

16

In the last expression we have used the relation $\text{Tr } AB = \text{Tr } BA$, which holds whenever AB is square. Expression (31) is invariant with respect to replacement of U by UB, where B is any nonsingular $k \times k$ matrix. In fact, the matrix $S_d U (U^T U)^{-1} U^T$ is unaffected by such a transformation. Furthermore, let J be an $m \times m$ symmetric positive definite matrix and let V be any $m \times k$ basis matrix. Since $V^T J V$ is positive definite, there exists [18] a real nonsingular upper triangular $k \times k$ matrix B^{-1} such that $V^T J V = (B^{-1})^T (B^{-1})$. Let $U = VB$. Then $U^T J U = B^T (V^T J V) B = I$. Thus any normalization of the form $U^T A U = I$ may be assumed without loss of generality. We suppose

$$U^T U = I. \tag{32}$$

Hence U must be found which maximizes $\text{Tr } \{U^T S_d U\}$ subject to the constraint (32). By partitioning U into individual columns of basis vectors and considering the maximization process involved, it can be shown [18] that the columns of U must be chosen as those eigenvectors corresponding to maximal eigenvalues $\lambda_1 \geq \ldots \geq \lambda_k > 0$ of S_d. Thus U must satisfy

$$S_d U = U \Lambda \quad , \tag{33}$$

where

$$\Lambda = \text{diag} [\lambda_1 \lambda_2 \ldots \lambda_k] \; .$$

17

Substituting (32) and (33) into (31) gives

$$E\{q_{min}(U)\} = TrS_d - Tr\Lambda = \sum_{i=k+1}^{k}\lambda_i \text{ for optimum } U.$$

The ratio
$$\alpha = \frac{\sum_{i=1}^{k}\lambda_i}{Tr S_d} \tag{34}$$

is sometimes called [8] the fraction of the total variance "explained" by the basis U.

It follows from (28) and (31) by us. the propagation rule for covariances, with $TrAB = TrBA$, that

$$E\{q_{min}(U)\} = TrS_{UC-d}.$$

Thus $E\{q_{min}(U)\}$ may also be given another interpretation. As a criterion of the size of the errors resulting from a distribution having zero mean and second moments defined by a given covariance matrix S, we may choose TrS. Since the trace is equal to the sum of the eigenvalues of a matrix, this interpretation is geometrically equivalent to defining the "size" of an m-dimensional ellipsoid as the sum of the squares of its semi-axes. The interpretation of $E\{q_{min}(U)\}$ as the trace of the covariance matrix will be freely used throughout the remainder of the report. Note that $E\{q_{min}(U)\}$ is also equal to m times the expected overall mean-square error of the approximation d ~ UC.

Although no use is made of the result in what follows, it is interest-
ing that the minimum of the quadratic form

$$q_d(U, C) = (d - UC)^T S_d^{-1}(d - UC)$$

has the expected value $m - k$ for _any_ choice of U, and therefore _cannot_
be used to determine an optimum basis.

From the preceding discussion it follows that an optimum basis
U for use with the integral equation would be that which minimizes

$$Tr S_{UC-\eta} = Tr \{S_f + T + T (XS_f X) T - TXS_f - S_f XT \} , \qquad (35)$$

From the definition of T we see that, even with the normalization
$U^T XU = I$, expression (35) is of fourth degree in the elements of U.
Since minimization of (35) is difficult, and since classical basis
vectors seem to suffice in practice, the determination of U from
(35) will not be pursued further in this paper.

5. Quality Criterion

The quantity TrX^{-1} can be used as a measure of the accuracy to be
expected from a given integral equation with given covariance matrices
S_f and S_ϵ and a given set $\{x_i\}$ of values of x. For $k = m$, i.e., for a non-
singular $m \times m$ matrix $U, S_{UC-\eta}$ reduces to X^{-1} by (23). Furthermore, as
demonstrated below, $Tr S_{UC-\eta} \geq TrX^{-1}$ for any basis U. Thus, TrX^{-1}
is a measure of the best that can be done for a given problem. Calcu-
lating TrX^{-1} and comparing with TrS_f indicates the amount of improve-
ment over the _a priori_ statistical knowledge that can be expected in a
given case.

19

Theorem: $\operatorname{Tr} S_{UC-r_i} - \operatorname{Tr} X^{-1} \geq 0$, where, as previously defined,

$$X = S_i^{-1} + A^T S_\varepsilon^{-1} A,$$

$$D = U^T X U,$$

$$T = U D^{-1} U^T,$$

$$\operatorname{Tr} S_{UC-r_i} - \operatorname{Tr} X^{-1} = \operatorname{Tr} \{ S_f + T + T X S_f X T - T X S_f - S_f X T - X^{-1} \}$$

$$U = \left[U_1 \Big| U_2 \Big| \dots \Big| U_k \right] \Big\} m$$ where the U_i are linearly independent

$\underbrace{}_{k}$

and $m \geq k$.

Lemma: $\operatorname{Tr} B^T S_f B \geq \operatorname{Tr} B^T X^{-1} B$ where B is any real $m \times m$ matrix.

Proof: Let $S_f = (S_{ij})$, $X^{-1} = (X_{ij}^{-1})$, and $B = (B_{ij})$. By direct calculation,

$$\operatorname{Tr} B^T S_f B = \sum_{i,p,q} B_{pi} S_{pq} B_{qi} = \sum_{i=1}^{m} \left(\sum_{p=1}^{m} \sum_{q=1}^{m} S_{pq} B_{qi} B_{pi} \right) = \sum_{i=1}^{m} B_i^T S_f B_i,$$

where B_i is the $i\underline{\text{th}}$ column vector of B. By an extension [19] of

Bergstrom's inequality we have, for any real column vectors y and z,

$$(y^T S_f y)(z^T S_f^{-1} z) \geq (y^T z)^2.$$

Since $X = S_i^{-1} + A^T S_\varepsilon^{-1} A$ so that $z^T X z \geq z^T S_f^{-1} z$, we have

$(y^T S_f y)(z^T X z) \geq (y^T z)^2.$ Putting $y = B_i$, $z = X^{-1} B_i$ gives

$(B_i^T S_f B_i)(B_i^T X^{-1} B_i) \geq (B_i^T X^{-1} B_i)^2.$ If $B_i \neq 0$, dividing out the positive

quantity $B_i^T X_i^{-1} B_i$ gives $B_i^T S_f B_i \geq B_i^T X^{-1} B_i$. (If $B_i = 0$, the in-

equality is trivially true.) Therefore,

$$\mathrm{Tr}\, B^T S_f B = \sum_{i=1}^{m} B_i^T S_f B_i \geq \sum_{i=1}^{m} B_i^T X^{-1} B_i = \mathrm{Tr}\, B^T X^{-1} B.$$ This proves

the lemma. It can now be applied to prove the theorem. Note that

$S_{UC-\eta} - X^{-1}$ may be written as $S_{UC-\eta} - X^{-1} = (XT - I)^T S_f (XT - I) +$

$T - X^{-1}$. By the lemma

$$\mathrm{Tr}\,\{S_{UC-\eta} - X^{-1}\} \geq \mathrm{Tr}\,\{(XT-I)^T X^{-1} (XT-I)\} + \mathrm{Tr}\, T - \mathrm{Tr}\, X^{-1}$$

$$= \mathrm{Tr}\,\{TXT - 2T + X^{-1} + T - X^{-1}\}.$$ Since $TXT = T$ we have

$$\mathrm{Tr}\,\{S_{UC-\eta} - X^{-1}\} \geq \mathrm{Tr}\, 0 = 0. \quad \mathrm{q.e.d.}$$

There are conditions for which a basis may be chosen such that

$\mathrm{Tr}\, S_{UC-\eta}$ decreases as k increases, and approaches $\mathrm{Tr}\, X^{-1}$ for k

considerably less than m. Such behavior is illustrated in figure 1,

which presents the values of $\mathrm{Tr}\, S_{UC-\eta}$ vs. k for the integral equation

(36), given and discussed in section 6. The conditions are:

$S_\epsilon = .01\, I$, $n = 7$, $m = 15$ with $\{x_i\}$ and $\{y_j\}$ as given in section

6. The Obukhov basis resulting from the S_f of table 1 is

used. Figure 2 presents the values of

21

$\text{TrS}_{UC-\eta}$ vs. k under similar conditions using the power basis $U_{ij} = y_i^{j-1}$ and figure 3 presents similar results for the trigonometric basis $U_{i,2j} = \sin\left(\frac{2\pi j y_i}{b-a}\right)$ $i = 1, 2, \ldots, 15$, $j = 1, 2, \ldots, 7$

$U_{i,2j+1} = \cos\left(\frac{2\pi j y_i}{b-a}\right)$ $i = 1, 2, \ldots, 15$, $j = 0, 1, 2, \ldots, 7$.

Evidently $k = 6$ will suffice for the power basis and $k = 11$ will suffice for the trigonometric basis. Figures 1, 2, and 3 are combined for easy comparison in figure 4.

The results of figures 1 through 4 arise from reasonably well-chosen bases. The type of behavior to be expected for ill-chosen bases is indicated in figures 5 and 6. Figure 5 presents $\text{TrS}_{UC-\eta}$ vs. k for a basis consisting of random numbers uniformly distributed between -1 and +1. Figure 6 presents similar results for the basis $U_{ij} = \delta_{ij}$. Clearly, in these cases nothing less than a full complement of basis vectors (i. e., $k = m = 15$) will achieve the desired accuracy. By noting that $\text{TrS}_{UC-\eta}$ is m times the theoretical overall mean-square error of the fit, we see that $\text{TrS}_f = 120.407$ corresponds to an overall rms error of 2.88 and that $\text{TrX}^{-1} = 23.946$ corresponds to an overall rms error of 1.26. This shows the extent to which the original statistics of f may be improved by using the integral equation in this particular case. The analysis presented here serves a similar purpose to the analysis of the "degree of independence" of the measurements of g(x) as discussed by Twomey [6], [11]. However, in the present

22

case the actual rms error to be expected is found and the results are necessarily dependent on the statistics S_ϵ and S_f, as well as on the kernel of the integral equation.

6. Numerical Inversion Results

For purposes of numerical experimentation the following equation was used:

$$e^{-\alpha(x)H_o} \alpha(x) \int_o^H e^{-y/H_o} f(y) e^{\alpha(x)H_o e^{-y/H_o}} dy = g(x). \qquad (36)$$

This equation occurs in remote atmospheric probing work if an exponential atmosphere is assumed. Here H_o is a constant and $\alpha(x)$ is given by

$$\alpha(x) = 1.1 x - 1 \qquad (37)$$

for the purposes of this section. If $f = f_c = $ const. is inserted in the left side of (36) and the integrations performed, the resulting right side is:

$$g(x) = f_c \left[1 - e^{-\alpha(x)H_o(1 - e^{-H/H_o})} \right] . \qquad (38)$$

Substituting (38) into (36) will, of course, give an integral equation whose correct solution is $f = f_c$. In the work reported here, the values $H = 10$, $H_o = 5$, and $f_c = 293.997$ were assumed. To study the

23

Table 1. COVARIANCE MATRIX OF 1

24

behavior of (36) in the presence of measurement error, random errors distributed in accordance with S_ϵ were added to g(x) as given by (38) and the mean value f_0 was varied randomly from f_c in a manner determined by S_f, which is given in Table 1.

Since the solution f simulates an atmospheric temperature profile, S_f was obtained from radiosonde data from 240 soundings during August at Denver, Colorado. The matrix S_ϵ was assumed to be scalar and the values assumed will be indicated. The method of constructing random errors is indicated below.

The CDC 3600 computer has a **FORTRAN** function, RANF (-1), which gives random numbers uniformly distributed between 0 and 1. These numbers are random in the same sense that a table of random numbers is random; that is, if the series of statements V_i = RANF(-1), i = 1, 2, ... M is repeated in the same manner, where i = 1 refers to the first use of RANF (-1) in a given computer run, the same sequence will result, but the sequence itself is random. It follows from the central limit theorem [20] that the variable $\hat{V}_M$, where

$$\hat{V}_M = \frac{\sum_{i=1}^{M} V_i - M/2}{\sqrt{M/12}} \tag{39}$$

is approximately a random normal deviate (i.e., it has a normal distribution with mean zero and standard deviation 1), the degree of the approximation depending on the size of M. A sample of 9,000 values of $\hat{V}_M$ was calculated for M = 1, 2, 4, 8, and 16.

Histogram frequencies were found and compared with the frequency distribution for random normal deviates. There appeared to be no significant discrepancy between the histogram and the theoretical curve for $M \geq 8$. In all work reported here $M = 10$ was used.

To simulate errors having a given covariance matrix S, we first determine [17] a matrix W such that

$$S = W^T W \quad . \tag{40}$$

If $V = (V_1, V_2, \ldots V_m)^T$ is a sample of independent random normal deviates, we form $\tilde{V} = W^T V$. Then, since $S_V = I$, it follows from the propagation rule for covariance matrices that

$$S_{\tilde{V}} = (W^T) I (W^T)^T = W^T W = S. \tag{41}$$

This process was used to simulate errors having zero mean and covariance matrix S_f.

In the simulation of errors the mean vector f_o was varied rather than the sample vector f because the integration to give the right side of (36) could then be obtained in closed form as (38), and a check on the accuracy of quadrature could also be obtained. A total of 15 quadrature abscissas were chosen; these consisted of 5 Gass-Legendre values for each of 3 intervals: 0 to 1, 1 to 3, and 3 to 10 respectively. Intervals of different length were needed because of

the general decaying-exponential character of the kernel. The interval enclosing the x_i was taken as $1 \leq x_i \leq 1.98$, $i = 1 \ldots n$. The x_i were evenly spaced, and the values used will be indicated. Under these conditions a numerical integration with Gaussian quadrature was compared (for $f = f_c$) with (38) and the maximum quadrature error was found to be .0011 in the right side, for which the actual value varied from about 103 to 292. All solutions used the classical Obukhov basis. In table 2 results are shown for $x_i = 1(.0544\ldots)1.98$, where the x_i are rounded to four decimal places. Here $n = 19$, $\alpha(x_i)$ is given by (37), S_f is as given in table 1, $S_\epsilon = \sigma_\epsilon^2 I = 10^{-4} \cdot I$, and $f_c = 293.997$ as indicated. The solutions were run with $k = 5$. Under these conditions $\text{Tr} S_{UC - \eta} = \text{Tr} X^{-1} = 12.8$. There was some loss of accuracy in the computation, so that trace values are good only to one decimal place. These were the only trace computations for which the computation errors were noticeable; most other trace values were computed using double precision. The overall rms error corresponding to $\text{Tr} X^{-1} = 12.8$ is .92. The solution of table 2 and two others are shown graphically in figures 7, 8, and 9. The three solutions were selected at random from a "run" of 40 solutions.

Table 2

SOLUTION #1 CF INTEGRAL EQUATION, $f_c = 293.997$;

SAMPLE RMS ERROR: 0.71

y	UC	$f = f_o \pm UC$	f_o
.046910077	-1.220	294.02	295.24
.23076534	-1.894	293.25	295.15
.50000000	-2.687	293.86	296.55
.76923466	-3.018	295.07	298.09
.95308992	-3.075	295.03	298.10
1.0938202	-3.066	294.89	297.95
1.4615307	-2.944	294.05	297.00
2.0000000	-2.475	293.85	296.33
2.5384693	-2.155	293.60	295.75
2.9061798	-1.844	293.44	295.28
3.3283705	-1.598	293.98	295.58
4.6153574	-1.157	292.94	294.10
6.5000000	-1.779	295.16	296.94
8.3846426	-2.332	293.55	295.89
9.6716295	-2.268	294.52	296.79

The index TrX^{-1} was computed for exactly the same conditions as for

the solutions of figures 7, 8, and 9 except that $S_\epsilon = \sigma_\epsilon^2 \cdot I = (.01) \cdot I$. Under

these conditions it was found that $TrX^{-1} = 21.44$. Next every second and

third value of x_i was removed to give the set $x_i = 1 (.1633...) 1.98$

where the resulting x_i are rounded to four decimals. In this case

$n = 7$ and $TrX^{-1} = 23.95$. This is the case shown in figure 1.

Decreasing n from 19 to 7 had very little effect on the expected error.

The effect of changing n is summarized in table 3. For this kernel,

the theoretical rms error is not strongly influenced by n, as long as

the interval (1, 1.98) remains fixed.

Table 3

TrX^{-1} FOR VARIOUS x-CONFIGURATIONS ON (1, 1.98)

n	x_i	TrX^{-1}	Theoretical Overall rms errors
19	1(.0544)1.98	21.44	1.20
7	1(.1633)1.98	23.95	1.26
2	1(.98) 1.98	27.45	1.35

Figures 10, 11, 12, and 13 present results for the conditions of table 3

with n = 7 and k = 4. These solutions were selected at random from

a "run" of 40 solutions. The improvement of the solution over the

statistical values is not as pronounced, because of the increase of σ_ϵ

from .01 to .1.

Table 4

TYPICAL SOLUTION OF INTEGRAL EQUATION FOR
VARIOUS VALUES OF k WITH $n = 7$ and $\sigma_e = 0.1$

$f_0 + UC$

y	k = 1	k = 2	k = 3	k = 4	k = 5	k = 6	k = 9	k = 12	k = 15
.047	294.218	294.016	294.012	294.126	294.072	294.070	294.072	294.072	294.072
.231	295.710	295.338	295.279	295.353	295.365	295.367	295.369	295.368	295.368
.500	294.900	294.550	294.478	294.470	294.493	294.494	294.490	294.491	294.491
.769	293.544	293.192	293.153	293.091	293.113	293.112	293.109	293.108	293.108
.953	293.395	293.104	293.095	293.020	293.038	293.037	293.035	293.034	293.034
1.094	293.115	292.895	292.902	292.822	292.834	292.833	292.833	292.832	292.832
1.462	293.033	292.937	292.979	292.892	292.887	292.886	292.891	292.891	292.891
2.000	293.146	293.219	293.305	293.241	293.217	293.217	293.220	293.221	293.221
2.538	292.684	292.936	293.068	293.033	293.004	293.004	293.004	293.003	293.003
2.906	292.432	292.786	292.933	292.922	292.894	292.395	292.890	292.889	292.888
3.328	292.639	293.118	293.295	293.310	293.287	293.288	293.280	293.281	293.281
4.615	295.179	295.953	296.155	296.246	296.275	296.275	296.287	296.287	296.287
6.500	293.284	294.923	294.845	294.931	294.952	294.951	294.942	294.942	294.942
8.585	293.519	296.201	295.528	295.559	295.553	295.552	295.545	295.545	295.545
9.672	293.805	296.935	295.811	295.780	295.757	295.758	295.761	295.761	295.761

30

The 40 solutions of which figures 10 through 13 are a sample were also run for $k = 1, 2, 3, 5, 6, 9, 12,$ and 15. The same sequence of random errors was used for each run of 40. A typical solution is shown in table 4 for various values of k. Table 4 shows typical behavior of the solution as k is varied. In this case, any value of k from 3 through 15 would have given essentially the same solution.

31

7. Absorption of Microwaves in the 10-150 GHz Frequency Band.

The Van Vleck-Weisskopf theory [21] was applied by Van Vleck [22], [23], to the absorption of microwave by oxygen and water vapor. The formula obtained by Van Vleck [22] for the absorption of O_2 is

$$\gamma = 10^6 (\log_{10} e) \frac{8\pi^3 \nu N_d R_{O_2} B}{c(3kT)^2}$$

$$\sum_N \{2|\nu_{N+} f(\nu_{N+}, \nu)||\mu_{N+}|^2 + 2|\nu_{N-} f(\nu_{N-}, \nu)|$$

(42)

$$|\mu_{N-}|^2 + F(\nu)''|\mu_{N_o}|^2 \} e^{-E_N/kT} ,$$

where the following notation has been introduced:

a) N_d is the total number of molecules per cubic centimeter and R_{O_2} is the fraction of the total which is O_2;

b) c, k, and ν are the speed of light, Boltzmann's constant, and the frequency of the imposed microwave, respectively;

c) f and F are form factors for the line shapes given below;

d) ν_{N+} and ν_{N-} are resonant frequencies of the transitions; (N_o labels the so called zero frequency transition)*

e) γ is the absorption in decibels per kilometer and is numerically equal to the product of the mass absorption coefficient times the dens

f) N runs over odd integers labeling certain rotational quantum states;

g) $|\mu_N|^2$ is the square of the matrix element dipole moment evaluated between appropriate angular momentum states;

h) B is a rotational constant whose magnitude is 1.44 cm^{-1}, and

---

*The transition frequencies for oxygen can be calculated with sufficient accuracy for the purposes of this report from the formulas in Townes and Schawlow [24].

32

i) E_N is the energy level of the Nth quantum state.

In (42) the expression of Van Vleck has been translated into the more modern notation and two of these equations are consolidated. Furthermore, VanVleck's expression is for pure oxygen. The fraction, R_{O_2}, of oxygen in the dry atmosphere is about 0.2. In the actual atmosphere, R_{O_2} varies slightly since the mixing ratio of water vapor also varies.

The form factors in (42) are given by

$$f(\nu_i, \nu) = \frac{\nu}{\pi \nu_i} \left[\frac{\Delta\nu}{(\nu_i - \nu)^2 + (\Delta\nu)^2} + \frac{\Delta\nu}{(\nu_i + \nu)^2 + (\Delta\nu)^2} \right] , \tag{43}$$

and

$$F(\nu) = \lim_{\nu_i \to 0} \left[\nu_i f(\nu_i, \nu) \right] = \frac{2\nu\Delta\nu}{\pi \left[\nu^2 + (\Delta\nu)^2 \right]} . \tag{44}$$

The matrix elements of the dipole moment can be calculated from formulas in Townes and Schawlow [24].

The formula for the absorption by water vapor at the 22.235 GHz resonant line in decibels per kilometer is given by Van Vleck [23] as

$$\gamma_{6_{-5} \to 5_{-1}} = 10^6 (\log_{10} e) \frac{8\pi^3 \nu N_d R_{H_2O}}{3\, G\, kT} |\mu_{6_{-5} \to 5_{-1}}|^2 e^{-E_{5,-1}/kT}$$

$$\tag{45}$$

$$\nu_{6_{-5} \to 5_{-1}} \qquad f(\nu_{6_{-5} \to 5_{-1}}, \nu)$$

and G is the rotational partition function given by

$$G = \sum_{J=0}^{\infty} \sum_{\tau=-J}^{J} \left[2 - (-1)^{|\tau|} \right] (2J+1) e^{-E_{J\tau}/kT} \tag{46}$$

The dipole moments and transition frequencies of H_2O may be calculated from formulas in the Appendices of Strandberg [25]. These are much more complicated than the corresponding calculations of O_2.

Equation (46) implies that other transitions are possible for the H_2O molecule. If the form factor in (43) were valid for these, then the absorption of each of these lines would have the same form as (45). These frequencies are much higher, in general, than the highest frequency of interest for this paper. Thus, an approximate formula for these contributions Y can be written as $Y_{Res.}$, given by

$$Y_{Res.} = K \rho \nu^2 \Delta\nu. \qquad (47)$$

The total Y due to H_2O is the sum of the contributions of (45) and (47).

The experimental values appropriate for the K and $\Delta\nu$'s for the Van Vleck equations will be discussed in the next section. The $\Delta\nu$ is derived in the VanVleck-Weisskopf theory from considering broadening to arise from the finite extension of the time between collisions. In fact, $2\pi\Delta\nu$ is the reciprocal of the mean time between collisions in the VanVleck-Weisskopf theory. If one had hard spherical molecules, the mean time between collisions could easily be calculated from kinetic theory [26]. However, molecules interact in a much more complicated way than can be described by the simple hard-sphere collision picture. A better approximation can be made by considering the molecular interactions to be more complicated functions of the separation than the hard-sphere approximation. This at least improves the temperature dependence of $\Delta\nu$.

34

The classical theory described above does not explain why different lines have different widths. One could account for this in the classical approximation by ascribing a different interaction between each state. No a priori knowledge from classical theory can supply this sort of information and it must be introduced as an additional set of assumptions if one is to proceed further via a classical mechanical calculation of line widths.

A partial quantum mechanical approach to the problem was given by Anderson as quoted in Tsao and Gurnutte, [27]. The translational motion in this calculation is treated as a classical mechanical problem, whereas the internal state transitions are treated as a quantum mechanical problem. In this picture $\Delta \nu$ is given by

$$\Delta \nu = n \, v \, \sigma \quad , \tag{48}$$

where

$$\sigma = 2\pi \int b \, db \, f(I, b) .$$

In (48), n is the number density of perturbers, v is the average relative velocity, b is the separation of the molecules at closest approach and $f(I, b)$ is the distribution function for cross section as a function of the internal coordinates, I, and b.

35

8. Least-Squares Analysis of Line Width Data

The absorption equations given in the last section, as developed by

VanVleck and Weisskopf [21], contain essentially one undetermined

parameter, the line width constant, $\Delta \nu/c$. Calculations of this quantity

are laborious and many uncertainties are present in such calculations.

Examples of such uncertainties are lack of knowledge of the exact form

of the molecular interaction, imprecise knowledge of molecular constants

(such as quadrapole moments) which enter into the theory of line broad-

ening, and the effect of higher order corrections to the perturbation

expansions.

As a check on theory, there are fortunately many experimental

results on line broadening and absorption coefficients for a variety of

conditions of pressure and temperature. For low pressures (around

10 to 20 mm of Hg), direct measurements of line widths can be made

since unresolved lines are well separated and there is very little line

shape asymmetry from the "negative frequency" portion of the VanVleck-

Weisskopf line shape. However, there is danger in extrapolating these

low pressure measurements to high pressures, especially if the individ-

ual lines are not well resolved at the higher pressures. A notable

example of this type of behavior is oxygen.

In the work reported in this section, the absorption data of various

researchers have been least-square analyzed to determine line widths

36

and, in the case of water vapor, line shape factors. A least-squares analysis applied to nonlinear equations (such as the VanVleck-Weisskopf equations) cannot, in general, be solved exactly; the solution must be determined iteratively by use of a reasonable first estimate to insure convergence.

The least-squares method used here may be described as follows. We wish to characterize N data points d_i, by a function f_i of n parameters p_j such that

$$\sum_{i=1}^{N} (d_i - f_i(p_1, p_2, \ldots p_n))^2 \, w_i = min , \tag{49}$$

where w_i = positive definite weight of the ith data point. It is assumed that "reasonable" first approximations to the parameters p_j are known. If these first approximations are labeled as $p_j^{(0)}$, then the functions f_i may be expanded in a Taylor series about $p_j^{(0)}$:

$$f_i(p_j) \doteq f_i(p_j^{(0)}) + \sum_{k=1}^{n} \frac{\partial f}{\partial p_k} (p_j^{(0)})(p_j - p_j^{(0)}) . \tag{50}$$

Let

$$J = \begin{bmatrix} \dfrac{\partial f_1}{\partial p_1} & \dfrac{\partial f_1}{\partial p_2} & \cdots & \dfrac{\partial f_1}{\partial p_n} \\[2ex] \dfrac{\partial f_2}{\partial p_1} & \dfrac{\partial f_2}{\partial p_2} & \cdots & \dfrac{\partial f_2}{\partial p_n} \\[2ex] \vdots & & & \\[2ex] \dfrac{\partial f_N}{\partial p_1} & \dfrac{\partial f_N}{\partial p_2} & \cdots & \dfrac{\partial f_N}{\partial p_n} \end{bmatrix} \updownarrow N , \tag{51}$$

$$\longleftarrow \text{---------} n \text{---------} \longrightarrow$$

and

$$r = [d_1 - f_1, d_2 - f_2, \ldots, d_N - f_N]^T \qquad (52)$$

= vector of residuals.

In (51) and (52), both the function f_i and its derivatives are to be evaluated at the original estimate $p_j^{(0)}$. Then minimizing (49) yields the matrix equation given by Strand [28].

$$\Delta p = p - p^{(0)} = (J^T \Gamma J)^{-1} J^T \Gamma r, \qquad (53)$$

where

$$\Gamma = \text{diag} (w_1, w_2, \ldots, w_N). \qquad (54)$$

Equation (53) is then iterated by reevaluating (51) and (52) at each stage of the iteration process.

Equation (53) was applied to the oxygen absorption data of Artman [29] and Crawford and Hogg [30] to determine the values of the line width constants for both the (+) and (-) transitions. The data of Artman were taken under laboratory conditions at $T = 300^\circ K$ and pressures of 1 atm, $\frac{1}{2}$ atm, and $\frac{1}{4}$ atm in air. Each of the above samples of data was taken at approximately 25 frequencies covering the range of 50 to 62 GHz.

Each piece of data was weighted with unit weight. The data of Crawford and Hogg were taken from transmission studies through the atmosphere at sea level pressures. As stated in their article, the approximate temperature range during the period of measurement was $0 \pm 3^{\circ}C$. Hence, as with most data taken in the field, the uncertainty of these data is greater than that of laboratory measurements. The results of the least-squares fit are shown in table 5. As has been discussed previously [31], the numerical values of the normalized line width parameter $(\Delta \nu/c)/P$ decrease with increasing pressure. A new feature, possibly of significance for line breadth theory, is that the line widths of the + transitions are consistently higher than those of the - transitions for all of the data examined. In addition, the data of Crawford and Hogg give higher values of the line width than a simple extrapolation using the usually assumed temperature dependence would indicate. This fact causes the authors to speculate that the interaction of H_2O with O_2 might give rise to the increase in oxygen line widths. Of course, the residual absorption of the 22 GHz and the 183 GHz H_2O lines might also appear in this analysis as an increase in line width, but because of the absence of relative humidity measurements while the absorption measurements were being taken, it was impossible to ascertain if this was the case. In any case, it would be useful if measurements were taken of oxygen line broadening in the presence of water vapor.

Table 5

Line Widths of Oxygen Determined by a least-squares Analysis of the Data

of Artman and of Crawford and Hogg

Pressure (atm)	$(\frac{\Delta\nu+}{c})/P$ (cm^{-1}/atm)	$(\frac{\Delta\nu-}{c})/P$ (cm^{-1}/atm)	σ_Y (dB/km)	Aver. Y (dB/km)
Data of Artman (T = 300° K)				
1	.0341	.0298	.605	8.56
$\frac{1}{2}$	.0405	.0363	.581	5.15
$\frac{1}{4}$	.0748	.0442	.509	2.85
Data of Crawford and Hogg (T = 273°K)				
1	.0515	.0441	.613	5.79

-40

The 22-GHz water vapor absorption data of Becker and Autler [32] were also analyzed, but in a slightly different fashion. For a fixed temperature, the water vapor absorption coefficient may be written [23]:

$$\frac{\gamma}{\rho} = c_1 \tilde{\nu}^2 \left\{ \frac{\Delta\nu/c}{(\tilde{\nu} - \tilde{\nu}_0)^2 + (\Delta\nu/c)^2} + \frac{\Delta\nu/c}{(\tilde{\nu} + \tilde{\nu}_0)^2 + (\frac{\Delta\nu}{c})^2} \right\} + c_2 \tilde{\nu}^2 \frac{\Delta\nu}{c}, \qquad (55)$$

where $\frac{\Delta\nu}{c} = a(1 + b\rho)$. From 66 measurements of $\frac{\gamma}{\rho}$ vs. ρ and ν, four-and five-parameter fits to the data were determined. The parameters determined were c_1, c_2, a, b, and, in addition, for the five-parameter fit $\tilde{\nu}_0$. The results are tabulated in table 6 . The initial estimates in all cases were taken from accepted values of these constants.

Note that the resonant frequency determined by the five-parameter fit is very close to the accepted value $.7417 \text{ cm}^{-1}$, which is determined by other means. The values of c_2 and b, which describe respectively the nonresonant contribution of the 183 GHz and higher lines and the effect of H_2O-H_2O line broadening, are both noticeably higher than the accepted values. Again, these facts could be of theoretical significance.

Surprisingly good consistency was obtained between the four-and-five-parameter determinations, considering that the data were somewhat noisy.

Table 6

Water Vapor Absorption Parameters Determined by a Least-Squares Analysis
of the Data of Becker and Autler Using the Form

$$\frac{\gamma}{\rho} = c_1 \tilde{\nu}^2 \left\{ \frac{\Delta\nu/c}{(\tilde{\nu}-\tilde{\nu}_0)^2 + (\Delta\nu/c)^2} + \frac{\Delta\nu/c}{(\tilde{\nu}+\tilde{\nu}_0)^2 + (\Delta\nu/c)^2} \right\} + c_2 \tilde{\nu}^2 \frac{\Delta\nu}{c}$$

where $\Delta\nu/c = a(1 + b\rho)$

Units: γ/ρ dB/km per g/m^3

$\Delta\nu/c$ cm^{-1}

   a cm^{-1}

   b $(g/m^3)^{-1}$

$\tilde{\nu}, \tilde{\nu}_0$ cm^{-1}

Four-Parameter Fit	Initial Estimate	10th Iteration
a	.087	.08478
b	.005	.00708
c_1	.004	.00361
c_2	.05	.06089

rms deviation in γ/ρ = .00114 dB/km per g/m^3
average γ/ρ = .0154 dB/km per g/m^3

Five-Parameter Fit	Initial Estimate	10th Iteration
a	.087	.08366
b	.005	.00710
c_1	.004	.00355
c_2	.05	.06204
$\tilde{\nu}_0$	.7417	.74380

rms deviation in γ/ρ = .00114 dB/km per g/m^3
average γ/ρ = .0154 dB/km per g/m^3

9. Application of Quality Criterion to Determine the Reduction
of the Variance of a priori Temperature Data by
Microwave Radiation Measurements

In recent work by Twomey [11] and Mateer [8], the information

content of radiation measurements has been discussed. In particular,

it was shown that for physically realistic smooth kernels, independent

information obtained from separate measurements is severely limited

due to ubiquitous measurement error. Twomey [11] goes further in

his analysis and determines, from a large number, p, of possible

measurements with a given noise level, the number of independent

pieces of information, ℓ , which can be found [11], and gives a pro-

cedure for determining optimum frequency locations for the ℓ measure-

ments ($\ell < p$). In many inversion problems, however, certain informa-

tion about the unknown function is known before any measurements are

made. This a priori knowledge is embodied in the mean and the

covariance matrix, both of which can be estimated from past data.

The information content of radiation measurements should be judged by

the improvement over the a priori knowledge.

As noted in section 5, the quantity TrX^{-1} can be used as a

measure of the overall accuracy to be expected from a given integral

equation with given covariance matrices S_f and S_ϵ and a given set

$\{x_i\}$ of x. Calculating $Tr X^{-1}$ and comparing with TrS_f indicate

the amount of improvement over the a priori statistical knowledge

that can be expected in a given case. It is important to realize,

however, that TrX^{-1} is not a panacea because no single number

can adequately describe $m(m+1)/2$ of them. More detailed informa-

tion, such as the amount of reduction of variance of the function at

various points, can only be obtained by comparison of S_f and X^{-1}.

The calculations of X^{-1} in this section have been carried out for

ground-based probing "looking up" and for an integral equation

determined by the Van Vleck equation (42) for microwave oxygen

absorption. The temperature and pressure structure used in calcu-

lating the absorption at each height were determined by assuming a

constant lapse rate of 6.5 $^\circ$K/km to determine the temperature and

by integrating the hydrostatic equation to determine the pressure.

The effect of non-linearities in the kernel due to fluctuations of the

temperature from the mean value has not been included in

this analysis. The water vapor absorption was assumed to be zero,

and surface temperature and pressure were taken as 0° C and 850 mb,

respectively. For simplicity the pressure dependence of the normalized

line width constant ($\Delta\nu/P$) was neglected and the values of

$$\left((\frac{\Delta\nu}{c})/P\right)_\pm = \begin{matrix} .0341 \\ .0298 \end{matrix} \ cm^{-1}/atm$$ were used for + and - transitions respec-

tively. The calculations at each frequency have been made assuming

monochromaticity, so that the degradation of information due to finite receiver bandwidth is not accounted for. This effect should be small, however, since the ratio of receiver bandwidth to pressure-broadened linewidth can be made quite small for microwave receivers. Because of the previous assumptions, the calculations involving X^{-1} are meant to be illustrative only.

Before presenting these calculations, we must give one more theoretical extension of the methods of sections 3,4, and 5. For a ground-based probing scheme, the value of the function at the lower point, a, can usually be measured directly. This constrained point should be used to modify the statistical estimation of the function and its uncertainty as given by X^{-1}. First, the constraint can be incorporated into the integral equation by using a quadrature formula (such as Gauss-Radau) which uses the value of the function at a, f(a), directly:

$$\int_a^b K(x, y) f(y) \, dy = \sum_{j=1}^m w_j K(x, y_j) f(y_j)$$

$$= w_1 K(x, a) f(a) + \sum_{j=2}^m w_j K(x, y_j) f(y_j) \tag{56}$$

Thus, by subtracting $w_1 K(x, a) f(a)$ from the measured quantity, g(x), a matrix equation to be solved for (m-1) components of the

45

function of f is obtained. Second, knowing f(a) reduces the uncertainty in all the other functional values. The new covariance matrix, $S_f^{(c)}$, of dimension $(m-1) \times (m-1)$, has elements

$$S_{ij}^{(c)} = S_{ij} - \frac{S_{1i} S_{1j}}{S_{11}}, \qquad i, j = 2, 3, \ldots, m;$$

where

$$S_f = (S_{ij}) \text{ and } S_f^{(c)} = (S_{ij}^{(c)}) . \tag{57}$$

For convenience, the matrix $S_f^{(c)}$ will be referred to in the following as the constrained covariance matrix. Furthermore, instead of the mean, $\bar{f}$, as the best a priori estimate of f, the effect of knowing f_1 modifies this optimum a priori estimate to $\hat{f}$ where

$$\hat{f}_i = \bar{f}_i + \frac{S_{i1}}{S_{11}} (f_1 - \bar{f}_1), \qquad i = 2, \ldots, m. \tag{58}$$

Equations (57) and (58) may be derived from linear regressions of the $(m-1)$ functional values f_2, f_3, ..., f_m as functions of the surface value f_1.

The two temperature covariance matrices and the corresponding means were obtained by ensemble averaging of 5 years of radiosonde data for the 2 months, February and August, at Denver, Colorado. The February and August averages were over 163 and 240 soundings, respectively. The temperatures, given at heights determined by the radiosondes, were interpolated linearly to determine values at the 15

desired quadrature points. (Gauss-Radau quadrature was used for the subinterval 0 to 1 km, while Gaussian quadrature was used in the subintervals 1 to 3 km and 3 to 10 km.) The means $\overline{T}(h_i)$, and elements of the covariance matrix, $S(h_i, h_j) \equiv S_{ij}$, were determined from

$$\overline{T}(h_i) = \frac{1}{N} \sum_{\alpha=1}^{N} T_\alpha(h_i), \tag{59}$$

and

$$S_{ij} = \frac{1}{N-1} \sum_{\alpha=1}^{N} \left(T_\alpha(h_i) - \overline{T}(h_i) \right) \left(T_\alpha(h_j) - \overline{T}(h_j) \right), \tag{60}$$

where N is the number of soundings, α is an index for each sounding, and $T_\alpha(h_i)$ is the temperature of the αth sounding at the height h_i. The constrained covariance matrix was then calculated using (57). The means of February and August are .given in table 7 and the constrained covariance matrices for February and August are given in tables 8 and 9, respectively. It may be of interest to compare the unconstrained covariance matrix for August, given in table 1, with the constrained matrix for the same month, table 9. The elements of the matrices differ considerably only below the 10th quadrature point (around 3 km).

Table 7

Five-year Mean Temperature Profiles at Denver, Colorado, for February and August.

i	h_i (km)	$\bar{T}(h_i)$ (Feb.) (^{o}K)	$\bar{T}(h_i)$ (Aug.) (^{o}K)
1	0.000	268.23	294.00
2	0.140	269.92	293.48
3	0.416	269.56	292.47
4	0.723	268.15	290.87
5	0.943	266.83	289.43
6	1.094	265.87	288.40
7	1.462	263.54	285.69
8	2.000	260.08	281.56
9	2.538	256.76	277.32
10	2.906	254.40	274.47
11	3.328	251.59	271.25
12	4.615	242.56	262.74
13	6.500	228.80	250.11
14	8.385	219.18	236.16
15	9.672	217.11	226.76

To determine the amount of reduction of the a priori temperature variance by microwave measurements of oxygen emission, calculations of X^{-1} were made for a set of frequencies which approximately cover the entire oxygen band. This set is shown in table 10.

Table 8

Temperature Covariance Matrix, in $(°K)^2$, of Denver, February, Radiosonde Data for the 2nd to 15th Quadrature Points with Constrained Surface Temperature.

8.96	9.68	9.25	8.99	8.78	8.27	7.39	6.59	6.53	6.77	7.05	5.81	-.36	-5.37
9.68	14.91	15.37	15.18	14.93	14.15	12.69	11.19	10.95	11.23	11.42	9.34	-.71	-7.90
9.25	15.37	17.78	17.82	17.65	16.89	15.25	13.55	13.33	13.68	13.59	11.12	-1.13	-8.55
8.99	15.18	17.82	18.28	18.22	17.74	16.18	14.49	14.26	14.60	14.49	12.14	-.72	-8.27
8.78	14.93	17.65	18.22	18.31	18.02	16.57	14.92	14.65	14.99	14.89	12.69	-.51	-8.12
8.27	14.15	16.89	17.74	18.02	18.58	17.80	16.37	16.04	16.39	16.31	14.03	.12	-7.58
7.39	12.69	15.25	16.18	16.57	17.80	18.87	18.21	17.88	18.23	17.91	15.62	1.56	-6.24
6.59	11.19	13.55	14.49	14.92	16.37	18.21	19.50	19.60	19.97	19.16	16.51	3.00	-4.49
6.53	10.95	13.33	14.26	14.65	16.04	17.88	19.60	20.38	21.07	20.34	17.44	3.86	-3.77
6.77	11.23	13.68	14.60	14.99	16.39	18.23	19.97	21.07	22.29	21.79	18.65	4.67	-3.06
7.05	11.42	13.59	14.49	14.89	16.31	17.91	19.16	20.34	21.79	25.07	22.27	7.45	-1.71
5.81	9.34	11.12	12.14	12.69	14.03	15.62	16.51	17.44	18.65	22.27	26.74	14.28	5.02
-.36	-.71	-1.13	-.72	-.51	.12	1.56	3.00	3.86	4.67	7.45	14.28	27.75	29.55
-5.37	-7.90	-8.55	-8.27	-8.12	-7.58	-6.24	-4.49	-3.77	-3.06	-1.71	5.02	29.55	53.27

Table 9

Temperature Covariance Matrix, in $(°K)^2$, of Denver, August, Radiosonde Data for the 2nd to the 15th Quadrature Points with Constrained Surface Temperature.

2.14	2.18	1.70	1.46	1.31	.97	.63	.42	.27	.12	.13	-.06	-.15	-.13
2.18	3.55	3.32	3.01	2.77	2.26	1.57	1.10	.80	.49	.21	.14	.19	.33
1.70	3.32	3.98	3.83	3.60	3.05	2.14	1.50	1.08	.66	.10	.08	.16	.25
1.46	3.01	3.83	3.88	3.72	3.25	2.33	1.68	1.23	.82	.25	.31	.38	.38
1.31	2.77	3.60	3.72	3.65	3.30	2.42	1.80	1.35	.94	.38	.50	.61	.57
.97	2.26	3.05	3.25	3.30	3.30	2.57	2.00	1.54	1.13	.54	.73	.91	.85
.63	1.57	2.14	2.33	2.42	2.57	2.41	2.09	1.70	1.38	.78	1.06	1.28	1.12
.42	1.10	1.50	1.68	1.80	2.00	2.09	2.13	1.92	1.73	1.24	1.63	1.78	1.47
.27	.80	1.08	1.23	1.35	1.54	1.70	1.92	1.96	1.93	1.48	1.94	2.03	1.65
.12	.49	.66	.82	.94	1.13	1.38	1.73	1.93	2.20	1.91	2.43	2.40	1.86
.13	.21	.10	.25	.38	.54	.78	1.24	1.48	1.91	3.80	3.70	3.44	2.56
-.06	.14	.08	.31	.50	.73	1.06	1.63	1.94	2.43	3.70	6.47	7.36	6.85
-.15	.19	.16	.38	.61	.91	1.28	1.78	2.03	2.40	3.44	7.36	12.07	13.42
-.13	.33	.26	.38	.57	.85	1.12	1.47	1.65	1.86	2.56	6.85	13.42	17.39

Table 10

Frequencies Used in Calculations of $Tr\, X^{-1}$

ν(GHz)

47.02650	52.02593	60.43505
47.22650	53.93117	61.80036
47.94917	55.22163	62.48631
48.45304	56.26466	62.68631
50.28294	58.44669	63.98631

The calculations of X^{-1} were run for both months, and for assumed rms brightness temperature measurement errors of .01 °K, .1 °K, and 1.0 °K. The entire matrix of X^{-1} for Denver, February, with $\sigma_\varepsilon = .01$ °K is shown in table 11.

The meaning of a 15x15 covariance matrix cannot be presented in simple form. A rough estimate of the standard deviation to be expected at each quadrature height is given by the square root of the corresponding diagonal element of the covariance matrix. These quantities are plotted as functions of height in figures 14 through 19. For ease of comparison, the error distributions to be expected in the constrained solution are shown in figures 20 and 21. The corresponding overall quality criterion, $Tr X^{-1}$, is tabulated in tables 12 and 13.

Table 11

Solution Covariance Matrix X^{-1}, in $(°K)^2$, for the 2nd to 15th Quadrature Points Using Denver, February, Radiosonde Data with Constrained Surface Temperature, $n=15$ and $\sigma_\varepsilon = .01\ °K$.

.06	-.13	.03	.06	.07	.06	-.01	-.07	-.06	-.05	.01	.07	-.05	-.06
-.13	.30	-.14	-.17	-.17	-.09	.10	.16	.10	.05	-.06	-.12	.12	.08
.03	-.14	.24	.10	.04	-.13	-.14	-.02	.08	.14	.06	-.11	-.04	.17
.06	-.17	.10	.20	.15	.01	-.17	-.12	.00	.05	.09	.01	-.09	-.03
.07	-.17	.04	.15	.20	.08	-.15	-.16	-.07	-.02	.08	.13	-.13	-.18
.06	-.09	-.13	.01	.08	.29	.02	-.23	-.26	-.23	.10	.24	-.14	-.32
-.01	.10	-.14	-.17	-.15	.02	.47	.05	-.23	-.33	-.13	.25	.07	-.33
-.07	.16	-.02	-.12	-.16	-.23	.05	.61	.40	.12	-.40	-.15	.33	.33
-.06	.10	.08	.00	-.07	-.26	-.23	.40	.65	.53	-.36	-.42	.35	.71
-.05	.05	.14	.05	-.02	-.23	-.33	.12	.53	.80	-.22	-.63	.27	1.09
.01	-.06	.06	.09	.08	.10	-.13	-.40	-.36	-.22	.83	-.49	-.28	.44
.07	-.12	-.11	.01	.13	.24	.25	-.15	-.42	-.63	-.49	2.13	-.89	-2.84
-.05	.12	-.04	-.09	-.13	-.14	.07	.33	.35	.27	-.28	-.89	1.84	-1.05
-.06	.08	.17	-.03	-.18	-.32	-.33	.33	.71	1.09	.44	-2.84	-1.05	9.56

Table 12

Traces of S_f and X^{-1} For Denver, February, for Various rms Measurement Errors, σ_ϵ

σ_ϵ (°K)	$Tr\,S_f(°K)^2$ Unconstrained	$Tr\,X^{-1}(°K)^2$ Unconstrained	$Tr\,S_f(°K)^2$ Constrained	$Tr\,X^{-1}(°K)^2$ Constrained
.01	615.22	20.85	310.70	18.19
.1	615.22	43.86	310.70	37.91
1.0	615.22	93.11	310.70	85.05

Table 13

Traces of S_f and X^{-1} for Denver, August, for Various rms Measurement Errors, σ_ϵ

σ_ϵ (°K)	$Tr\,S_f(°K)^2$ Unconstrained	$Tr\,X^{-1}(°K)^2$ Unconstrained	$Tr\,S_f(°K)^2$ Constrained	$Tr\,X^{-1}(°K)^2$ Constrained
.01	120.48	5.73	68.92	4.76
.1	120.48	14.23	68.9_	12.67
1.0	120.48	33.91	68.92	31.61

The study of X^{-1} and its trace can be directed towards an important experimental consideration i.e.; namely, that of determining an optimum distribution of measurement frequencies, given that only a certain number of them (usually small) will be available. This problem has been studied by Twomey [11] from the point of view that the optimum location of measurements is determined by the integral equation itself. Further, from the analysis of a certain matrix, which depends on the kernel, he shows that the number of independent pieces of information is limited by the number of eigenvalues which are larger than the noise level of the measurements. In the absence of additional information, the above approach seems reasonable.

When additional information is available, such as the statistical information contained in S_f, it is clear that the optimum frequencies should be determined from a statistical compromise among S_f, S_e, and the properties of $A^T A$. This optimum set could be different for periods of different meteorological statistics. If the measuring instrument(s) is (are) not tuneable, a heterogeneous ensemble averaging over yearly data might be in order. A method which properly weights all available information has the advantage of allowing the choice of frequencies such that the duplication of easily available information (that of S_f and $\bar{f}$) by difficult experimental measurements is made as small as possible. The concept of "number of

independent pieces of information" is not as straightforward with this analysis as it was in Twomey's. However, an "effective number", such as the number of measurements required to reduce the a priori variance to a desired level, given that the noise level is fixed, can be defined. In a theoretical sense, such a number could always be obtained for any given level greater than zero since duplicating measurements is equivalent to lowering the noise level. Practically speaking, if a reasonably large reduction in variance with a few well-placed measurements is not possible, the experiment is probably impractical.

An attempt was made to determine the approximate sensitivity of $\text{Tr} X^{-1}$ to choice of and number of frequencies for one, two, and three frequencies and for $\sigma_\epsilon = .01^\circ K$. The one-frequency search was carried out starting with 47.0 GHz and adding a .5 GHz increment until 56 GHz was reached. These results, for both the constrained and unconstrained data, are shown in table 14 for the Denver, August, statistics.

The frequencies corresponding to the minimum trace are 54.5 GHz for the unconstrained (U) case ($\text{Tr} X^{-1} = 50.6\ (^\circ K)^2$) and 4.75 GHz for the constrained (C) case ($\text{Tr} X^{-1} = 37.7\ (^\circ K)^2$). The traces of S_f were 120.5 (C) and 68.9 (U), $(^\circ K)^2$, and the traces of X^{-1} for the 15 frequencies of table 10 were $5.7 (^\circ K)^2$ (U) and $4.8 (^\circ K)^2$ (C). Thus

55

Table 14

Trace X^{-1} vs. Frequency, Denver, August $\sigma_c = .01\,^\circ K$

(Single Frequency, $n = 1$)   Trace $S_f = 120.48$

ν (GHz)	$Tr\,X^{-1}(^\circ K)^2$ Unconstrained	$Tr\,X^{-1}(^\circ K)^2$ Constrained
47.5	60.3	37.7
48.0	56.9	39.2
48.5	55.4	39.9
49.0	54.8	40.2
49.5	54.5	40.4
50.0	54.2	40.6
50.5	53.9	40.7
51.0	53.6	40.9
51.5	53.2	41.2
52.0	52.8	41.5
52.5	52.3	41.9
53.0	51.8	42.4
53.5	51.2	43.1
54.0	50.7	44.2
54.5	50.6	45.6
55.0	51.0	47.0
55.5	51.8	48.3
56.0	52.7	49.4

the use of a single frequency, with this choice of σ_ϵ, reduces the variance by a factor of 2 (roughly).

The two-frequency calculations were done by fixing $\nu_1 = 47$ GHz and varying the second frequency, ν_2, from 48.3 GHz to 60.0 GHz in 1.3 GHz increments. These results are shown in table 15, which indicates that the variance obtained from the one-frequency calculations is roughly halved by the addition of the second frequency.

The three-frequency calculations were done by fixing $\nu_1 = 47$ GHz and $\nu_2 = 50.9$ GHz and varying the third frequency, ν_3, from 47.5 to 58.0 in .5 GHz increments. These results, again for Denver, August, and $\sigma_\epsilon = .01\,^\circ K$, are shown in table 16. It should be observed that $\operatorname{Tr} X^{-1}$ is approaching that of the 15-frequency calculations, and that addition of more frequencies will yield diminishing returns. The relative minimum of $\operatorname{Tr} X^{-1}$ at 47.5 GHz is presumably due to the nearby resonant line at 47.4465 GHz. A rigorous search for optimum frequencies would necessarily examine the effect of each resonant line on $\operatorname{Tr} X^{-1}$.

Table 15

Two-Frequency Calculations of $\text{Tr}\,X^{-1}$ for Denver,
August, $\sigma_c = .01\ ^\circ K$, $\nu_1 = 47.0$ GHz

ν_2 (GHz)	$\text{Tr}\,X^{-1}$ Unconstrained	$\text{Tr}\,X^{-1}$ Constrained
48.3	22.3	18.1
49.6	21.9	17.7
50.9	21.6	17.4
52.2	21.5	17.4
53.5	21.8	17.9
54.8	22.6	19.0
56.1	24.3	21.0
57.4	26.2	23.3
58.7	27.4	24.8
60.0	27.9	25.3

Table 16

Three-Frequency Calculations of $Tr\, X^{-1}$ for Denver, August,

$\nu_1 = 47$ GHz, $\nu_2 = 50.9$ GHz, $\sigma_\epsilon = .01\, ^\circ K$

ν_3 (GHz)	$Tr\, X^{-1}$ Unconstrained	$Tr\, X^{-1}$ Constrained
47.5	15.4	11.8
48.0	21.4	17.3
48.5	21.4	17.2
49.0	21.5	17.2
49.5	21.5	17.3
50.0	21.5	17.3
50.5	21.5	17.3
51.0	21.5	17.3
51.5	21.4	17.2
52.0	21.1	17.0
52.5	20.4	16.4
53.0	19.2	15.3
53.5	17.8	14.0
54.0	16.5	12.9
54.5	15.6	12.2
55.0	15.1	11.8
55.5	14.9	11.7
56.0	14.9	11.9
56.5	15.0	12.2
57.0	15.1	12.5
57.5	15.3	12.8
58.0	15.4	13.0

10. Summary

A method for the numerical solution of a Fredholm integral equation of the first kind has been derived and illustrated. The method requires knowledge of the covariance matrices of the constraint vector and the measurement error vector. Such knowledge is frequenctly available in physical problems when it is desired to derive values of physical functions from integrals involving them. If both covariance matrices S_f and S_ϵ are scalar, the equations reduce to those of Twomey [6], where the optimum smoothing parameter γ is given by the ratio of variances between the diagonal elements of S_ϵ and S_f, respectively. The present method automatically incorporates the optimum amount of smoothing in the sense of maximum-likelihood estimation.

The trace of the error covariance matrix, $\text{Tr} S_{UC-\eta}$, is used to estimate the precision of the solution. When $k = m$ (i.e., when the basis forms a nonsingular $m \times m$), $S_{UC-\eta}$ reduces to $X^{-1} \equiv (S_f^{-1} + A^T S_\epsilon^{-1} A)^{-1}$. The positive number $\text{Tr} X^{-1}$ is related to the error to be expected in the solution and is used as a quality criterion. A comparison of $\text{Tr} X^{-1}$ with $\text{Tr} S_f$ indicates the amount of information contained in the integral equation with observation errors determined by S_ϵ. It is evident that $\text{Tr} X^{-1}$ can be used to study

optimization of the spacing of observations. Such a study could be valuable for planning measuring systems.

The method of estimation and the use of the quality criterion $Tr X^{-1}$ were illustrated by studying the effect of various sequences of random errors on the solution of a specific integral equation. The effect of varying the number and type of basis vectors was studied for this example. The results apparently agree with theoretical predictions, although confidence tests were not run.

Calculations of X^{-1} and its trace were then performed using certain meteorological statistics of Denver, Colorado, and absorption coefficients determined from the Van Vleck absorption equations for the microwave oxygen complex with a linear temperature profile. These calculations were performed for a set of 15 frequencies selected to cover the oxygen band, and for three sets of assumed brightness-temperature rms errors of $.01\,^{\circ}K$, $.1\,^{\circ}K$, and $1.0\,^{\circ}K$. The square roots of the diagonal elements of X^{-1} were plotted as functions of height in an attempt to show the accuracy with which various parts of the tropospheric temperature profile could be

inferred from ground-based measurements of oxygen emission. Questions of optimum choice of frequencies for this probing were discussed and illustrative calculations relevant to this choice were presented.

11. Acknowledgements

12. References

1. Fleming, H. E., and D. Q. Wark (1965), A numerical method for determining the relative spectral response of the vidicons in a nimbus satellite system, Appl. Optics 4, No. 3, 337-342.

2. Kaplan, L. D. (1959), Inference of atmospheric structure from remote radiation measurements, J. Optical Soc. of Amer. 49, No. 10, 1004-1007.

3. King, J. I. F. (1964), Inversion by slabs of varying thickness, J. Atmospheric Sci., 21, 324-326.

4. Phillips, D. L. (1962), A technique for the numerical solution of certain integral equations of the first kind, J. Assoc. Comp. Mach. 9, 84-97.

5. Twomey, S. (1963), On the numerical solution of Fredholm integral equations of the first kind by the inversion of the linear system produced by quadrature, J. Assoc. Comp. Mach. 10, 79-101.

6. Twomey, S. (1965), The application of numerical filtering to the solution of integral equations encountered in indirect sensing measurements, J. Franklin Institute, 279, No. 2, 95-109.

7. Twomey, S. and H. B. Howell (1963), A discussion of indirect sounding methods with special reference to the deduction of vertical ozone distribution from light scattering measurements, Mon. Wea. Rev., 91, 659-664.

8. Mateer, Carlton L. (1965), On the information content of Umkehr observations, J. Atmospheric Sci., 22, 370-381.

9. Alishous, J. C., L. J. Crone, H. E. Fleming, F. L. Van Cleef, and D. Q. Wark (1965), A discussion of empirical orthogonal functions and their application to vertical temperature profiles, submitted to Tellus.

10. Wark, D. Q., and H. E. Fleming (1966), Indirect measurements of atmospheric temperature profiles from satellites: I. Introduction, Mon. Wea. Rev. 94, No. 6, 351-362.

11. Twomey, S. (1966), Indirect measurements of atmospheric temperature profiles from satellites: II. Mathematical aspects of the inversion problem, Mon. Wea. Rev., 94, No. 6, 363-366.

12. Kondrat'yev, K. Ya (1965), Radiative Heat Exchange in the Atmosphere, Translated by O. Tedder (Pergamon Press, New York).

13. Goody, R. M. (1964), Atmospheric Radiation (Oxford, Claredon Press).

14. Westwater, E. R. (1965), Ground-based passive probing using the microwave spectrum of oxygen, Radio Sci. J. Res. NBS, 69D, No. 9, 1201-1211.

15. Deutsch, Ralph (1965), Estimation Theory (Prentiss-Hall, Englewood Cliffs, New Jersey).

16. Obukhov, A. M. (1960), The statistically orthogonal expansion of empirical functions, Akademiya Nauk, SSR Izvestiya Seriya Geofizicheskaya, No. 3, 432-439, English translation by the Am. Geophys. Un., Nov. 1960.

17. Faddeeva, V. N. (1959), Computational Methods of Linear Algebra (Dover, New York) 81-85.

64

18. Courant, R. and D. Hilbert (1953), Methods of Mathematical Physics, Vol. 1, Interscience, 23-27.

19. Beckenbach, E. F. and R. Bellman (1961), Inequalities (Springer-Verlag, Berlin), Theorem 12, 69.

20. Cramér, H. (1946), Mathematical Methods of Statistics (Princeton, N.J.), 213-220.

21. Van Vleck, J. H. and V. F. Weisskopf (1945), On the shape of collision-broadened lines, Rev. Mod. Phys. 17, Nos. 2 and 3.

22. Van Vleck, J. H. (1947a), The absorption of microwaves by oxygen, Phys. Rev. 71, No. 7, 413-424.

23. Van Vleck, J. H. (1947b), The absorption of microwaves by uncondensed water vapor, Phys. Rev. 71, No. 7, 425-433.

24. T. wnes, C. H. and A. L. Schawlow (1955), Microwave Spectroscopy (McGraw-Hill, New York, N.Y.

25. Strandberg, M. W. P. (1954), Microwave Spectroscopy, Methuen's Monographs on Physical Subjects.

26. Kennard, E. H. (1938), Kinetic Theory of Gases (McGraw-Hill, New York, N. Y.).

27. Tsao, C. J. and B. Curnutte (1954), Line widths of pressure broadened spectral lines, Publication of Ohio State University Res. Foundation.

28. Strand, O. N. (1963), Determination of parameters for correlated data by the use of a generalized least-squares criterion using linearized residuals, U.S. Naval Ordnance Test Station, Report 7942, April, China Lake, California.

29. Artman, J. O. (1953), Absorption of microwaves by oxygen in the millimeter wavelength region, Columbia Radiation Laboratory Report, June, Columbia University, New York, N. Y.

30. Crawford, A. B. and D. C. Hogg (1956), Measurement of atmospheric attenuation of millimeter wavelengths, The Bell System Tech. J. 35, 907-916.

31. Abbott, R. L. (1964), Width of the microwave lines of oxygen and their relationship to the thermal noise emission spectrum of the atmosphere, Proc. 3rd Symp. on Remote Sensing of the Environment, Univ. of Mich., Ann Arbor, Michigan.

32. Becker, G. E. and S. H. Autler (1946), Water vapor absorption of electromagnetic radiation in the centimeter wave-length range, Phys. Rev. 70, 5, 300-307.

$TrS_{UC} - \eta$ vs. k for Obukhov basis. $n = 7$, $m = 15$,

$S_\epsilon = .01\,I$, S_f as in table 1.

$TrS_f = 120.407$

$TrX^{-1} = 23.946$

$k \longrightarrow$

Fig. 1

Tr $S_{UC}-\eta$

67
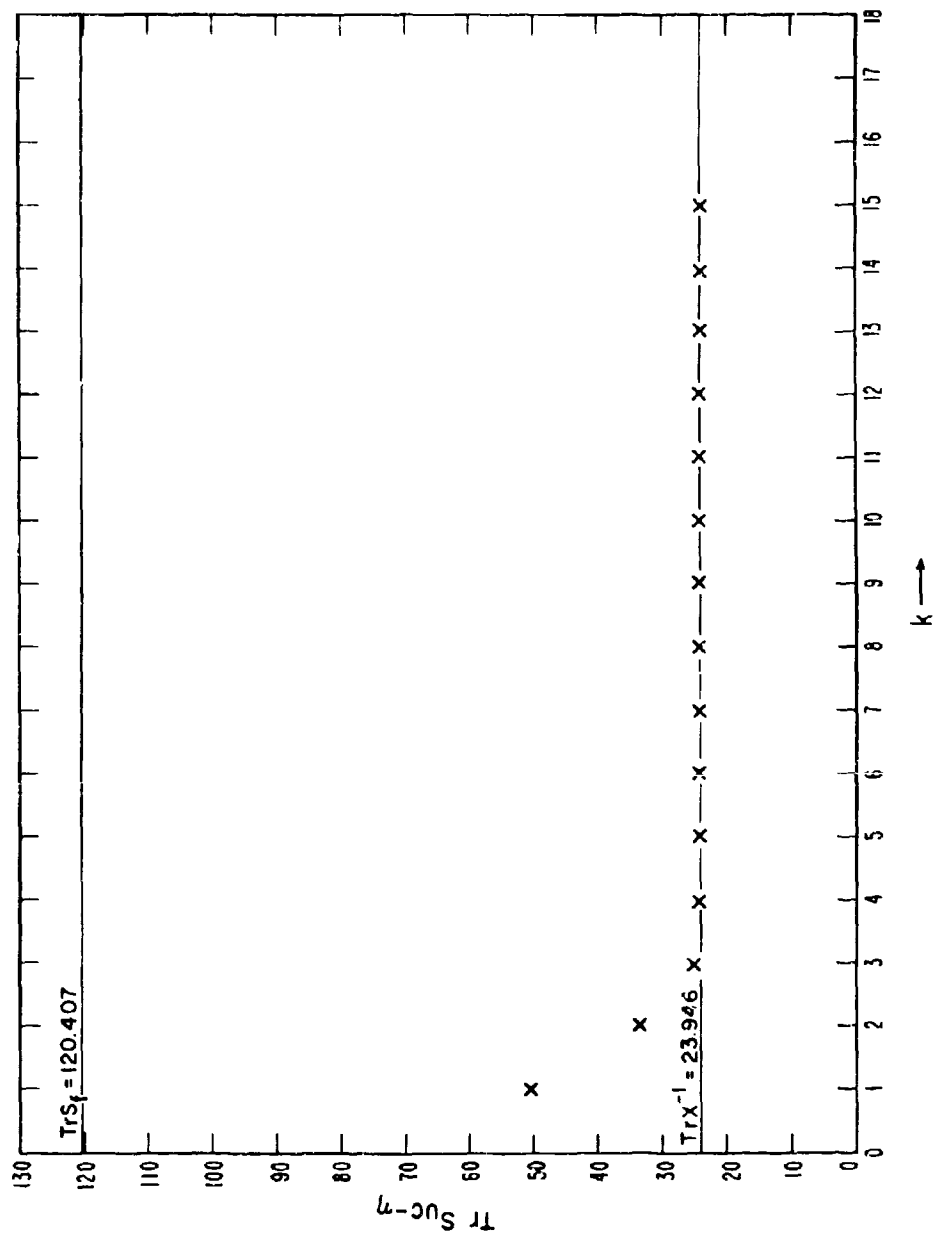
$TrS_{UC-\eta}$ vs. k for power basis. n = 7, m = 15.

$S_\epsilon = .01 I$, S_f as in table 1.

$TrS_f = 120.407$

$TrX^{-1} = 23.946$

Tr $S_{UC-\eta}$

k ⟶
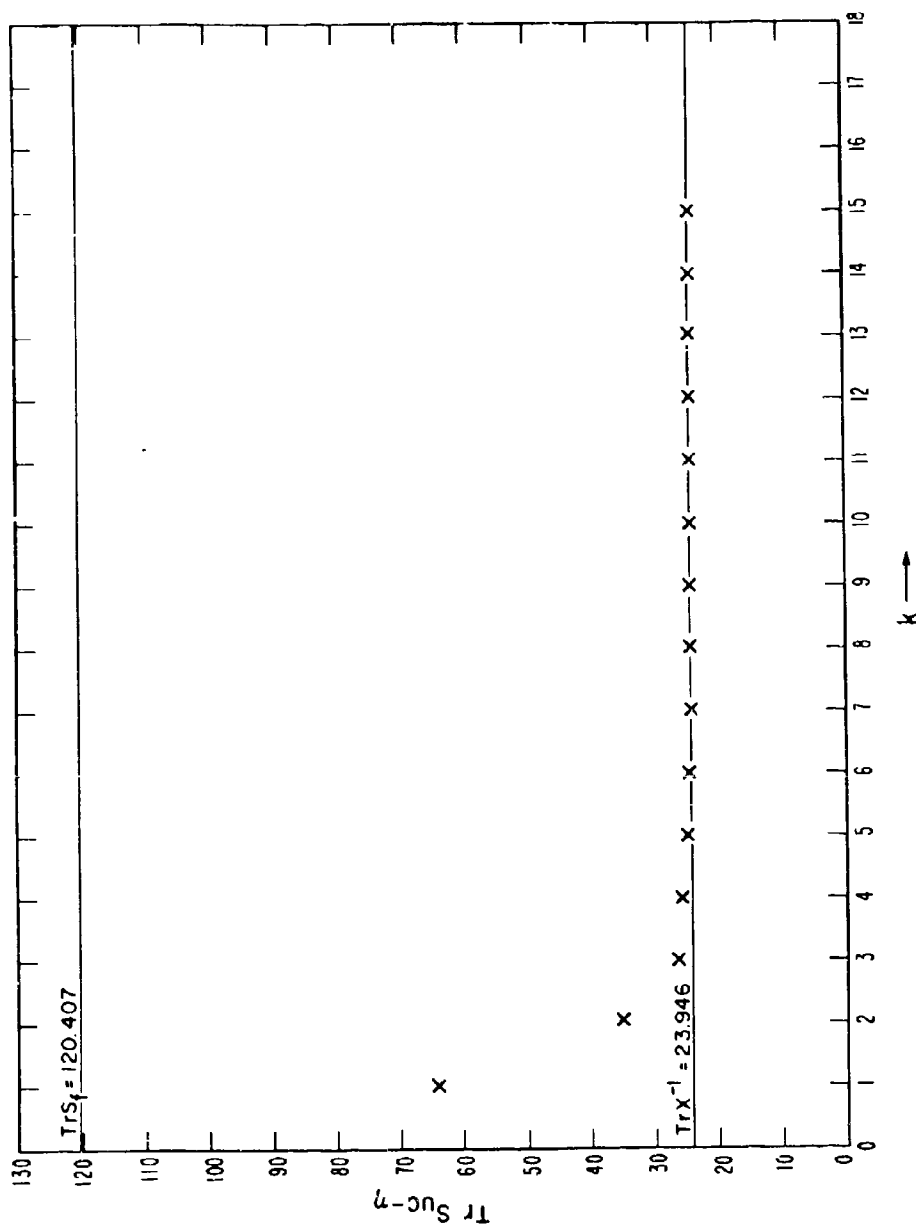
Fig. 2

$TrS_{UC-\eta}$ vs. k for trigonometric basis. $n = 7$, $m = 15$,

$S_\varepsilon = .01 I$, S_f as in table 1.

Fig. 3

69
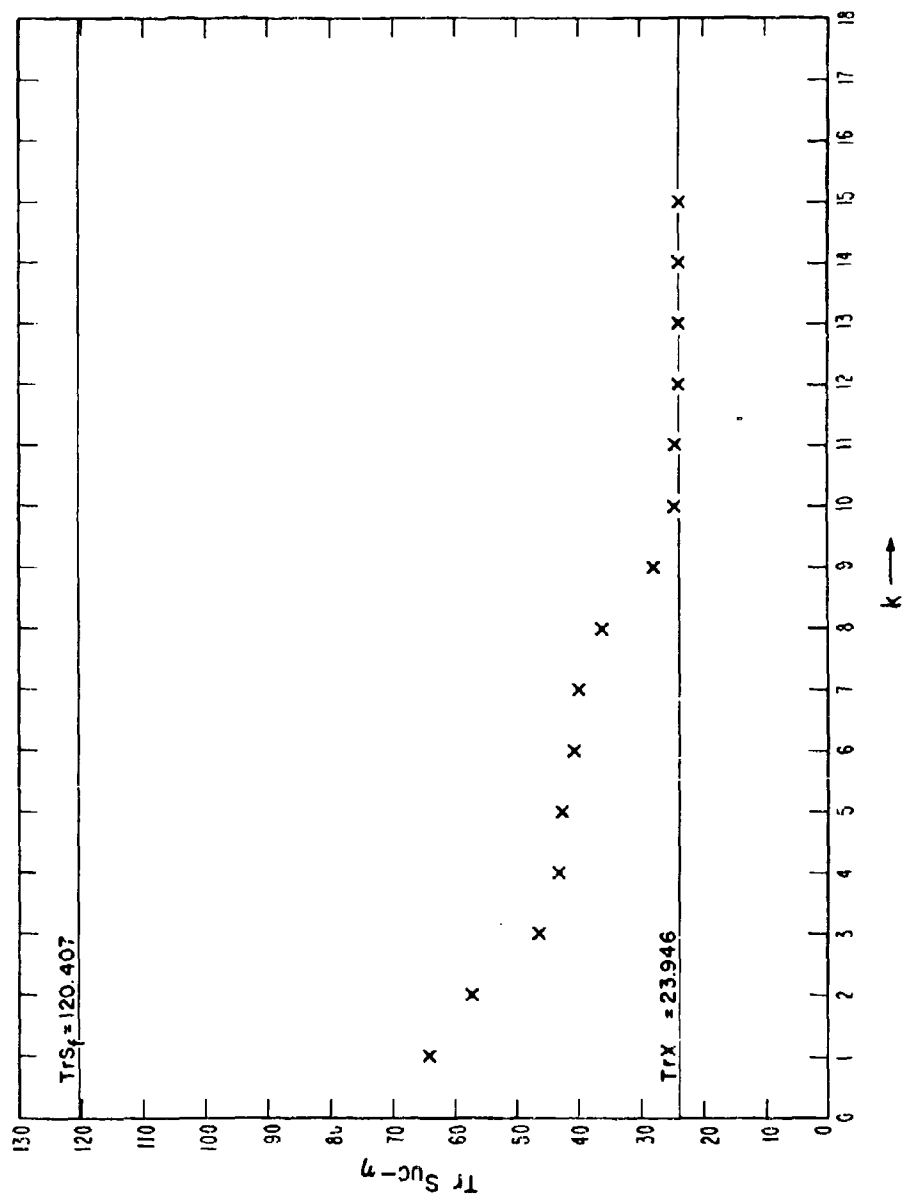
$TrS_{UC} - $ vs. k for three different bases   n=7, m=15,

$S_c = .01\,I$, S_f as in table 1.

OBUKHOV BASIS
POWER BASIS
TRIGONOMETRIC BASIS

$TrS_f = 120.407$

$TrX^{-1} = 23.946$

$Tr\,S_{UC}-\eta$

k ⟶

Fig. 4

70
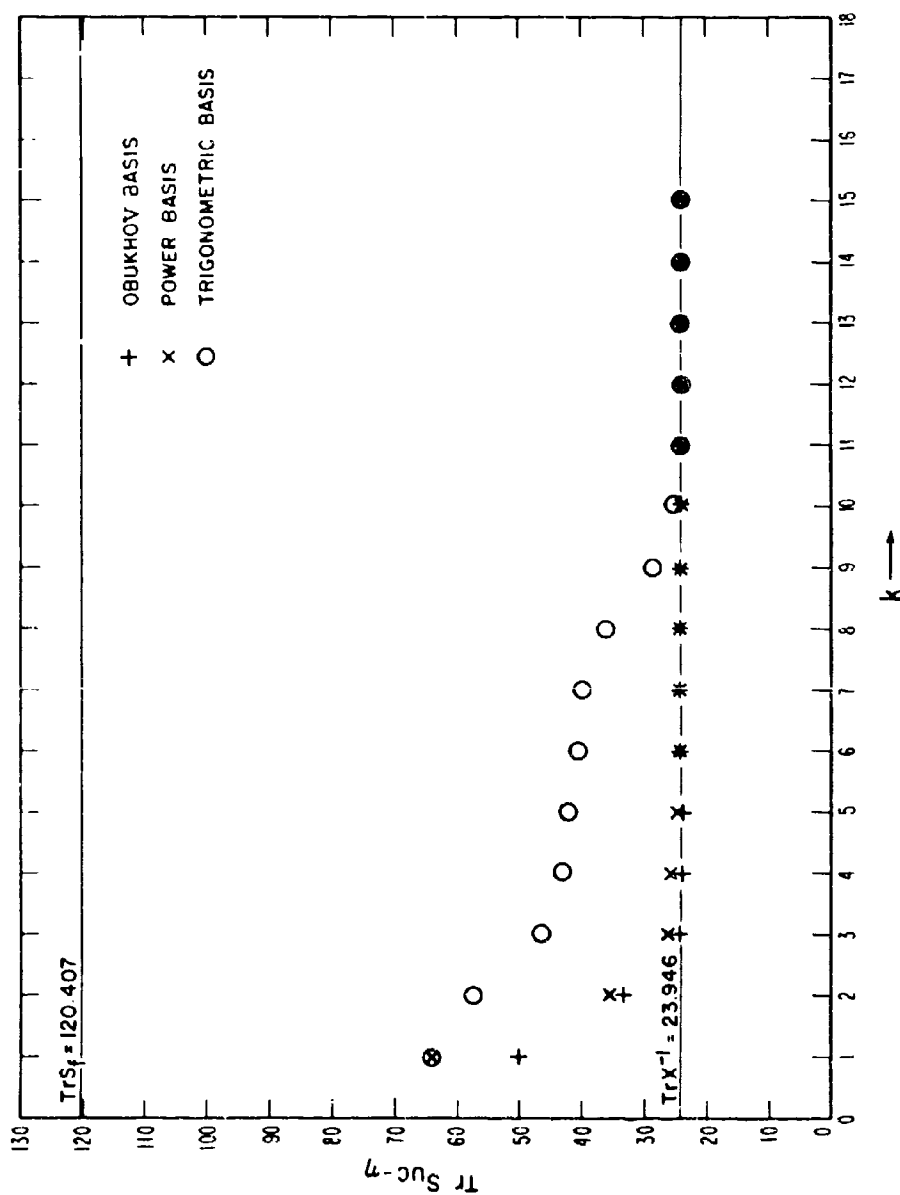
TrS_{UC-n} vs. k for a basis consisting of randomly-chosen numbers from a uniform distribution between -1 and +1.

$n = 7$, $m = 15$, $\xi_\epsilon = .011$, S_f as in table 1.

$TrS_f = 120.407$

$TrX^{-1} = 23.946$

Fig. 5

71
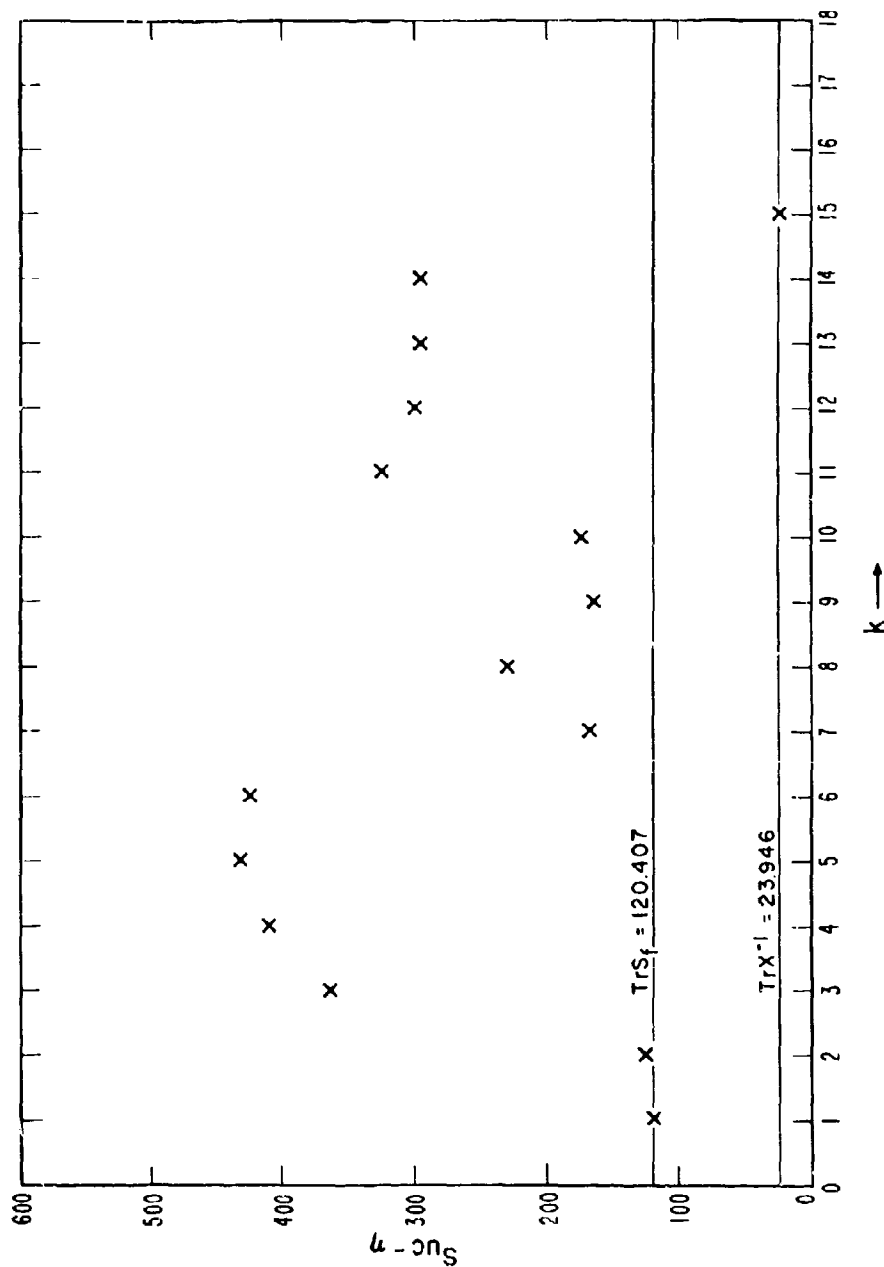
$\text{Tr}S_{UC-n}$ vs. k for the "unit" basis $U_{ij} = \delta_{ij}$.

$n = 7$, $m = 15$, $S_\epsilon = .011$, S_f as in table 1.

$\text{Tr}S_f = 120.407$

$\text{Tr}X^{-1} = 23.946$

S_{UC-n}

$k \longrightarrow$
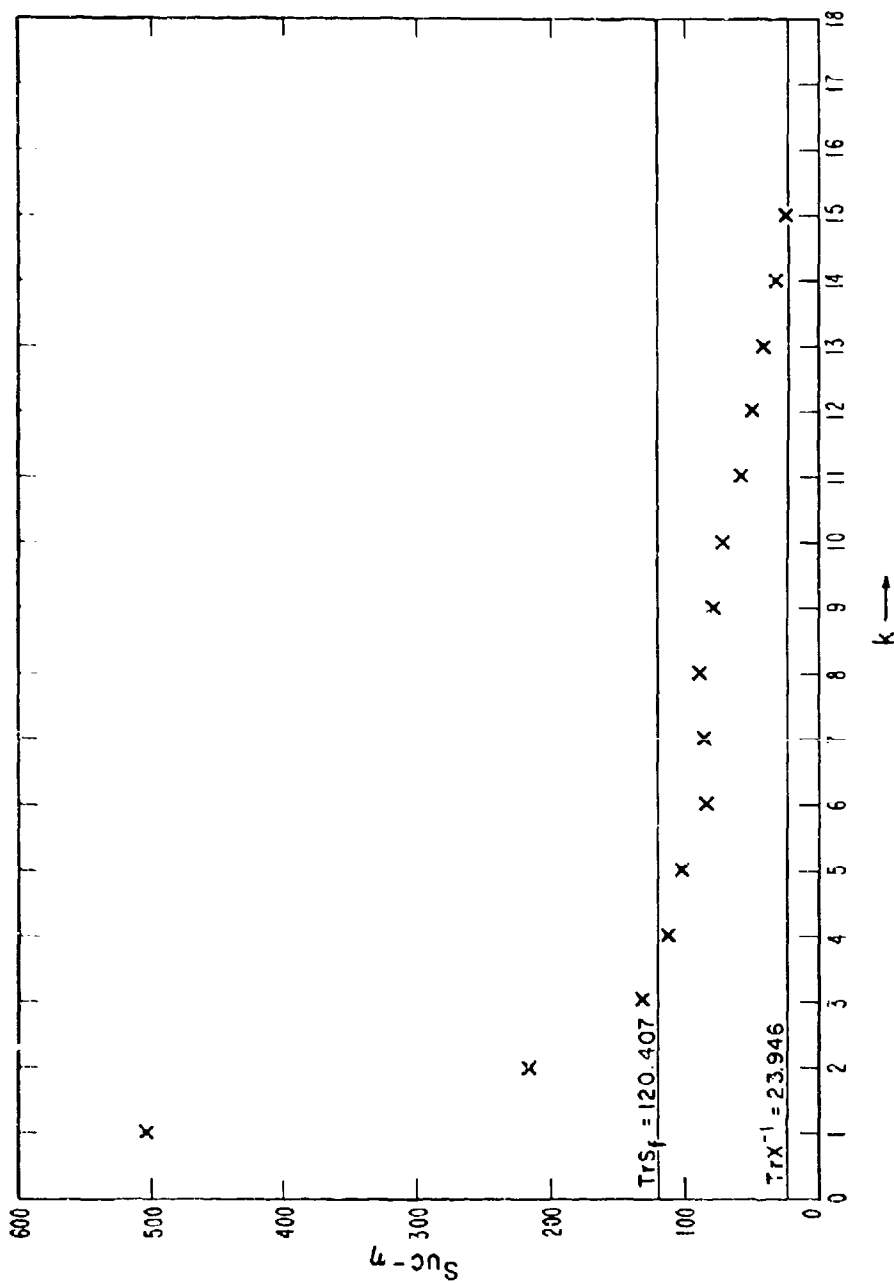
Fig. 6

Solution #1 of integral equation. Sample rms solution

error $= 0.7$, $S_c = 10^{-4} L$, S_f as in table 1, $k=5$, $n=19$,

$1 \leq x_i \leq 1.98$.

+ RANDOMLY-DETERMINED f_o
× STATISTICALLY-ESTIMATED SOLUTION $f_o + UC$

$f_c = 293.997$

f_o

$f_o + UC$

SOLUTION, DEGREES

y, km
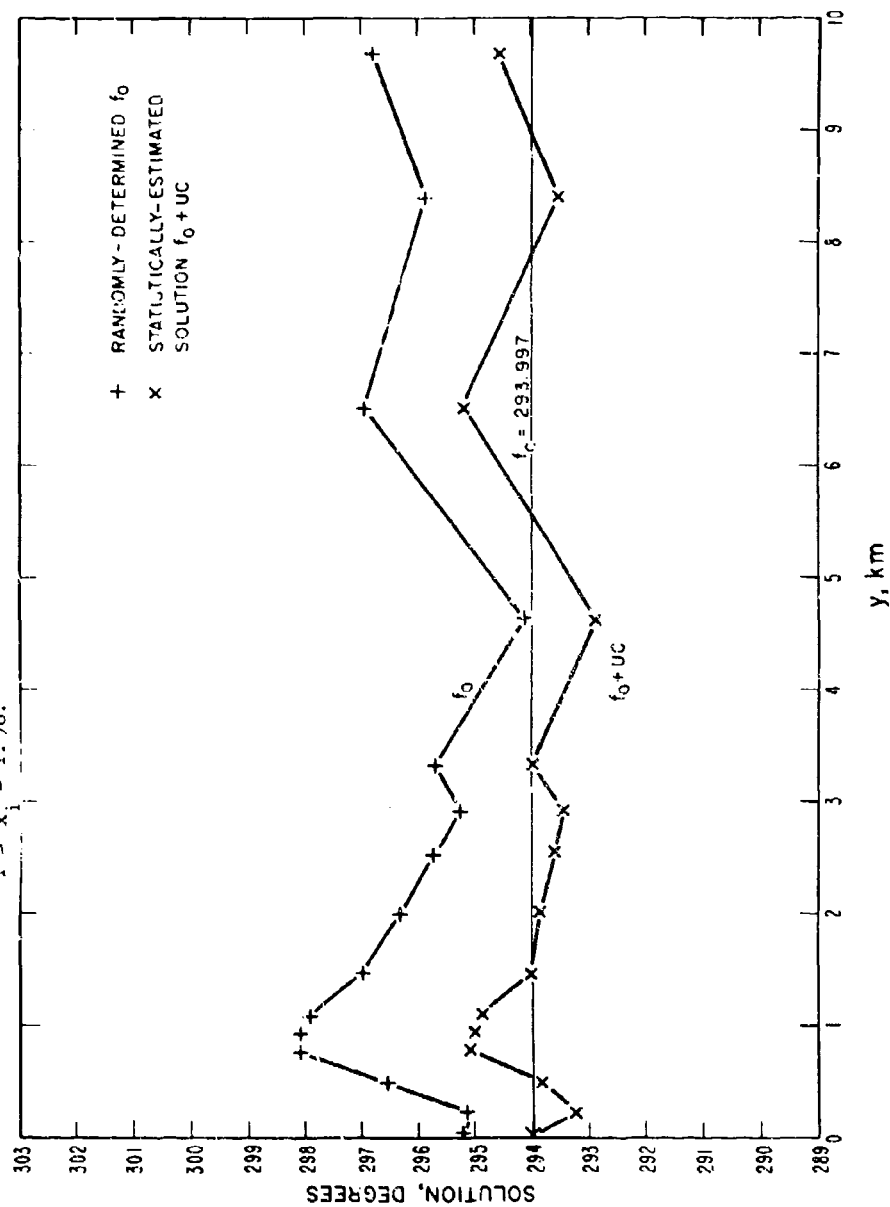
Fig. 7

Solution #2 of integral equation. Sample rms solution

error $= 0.4$, $S_{\epsilon} = 10^{-4}$ I, S_f as in table 1, $k = 5$, $n = 19$,
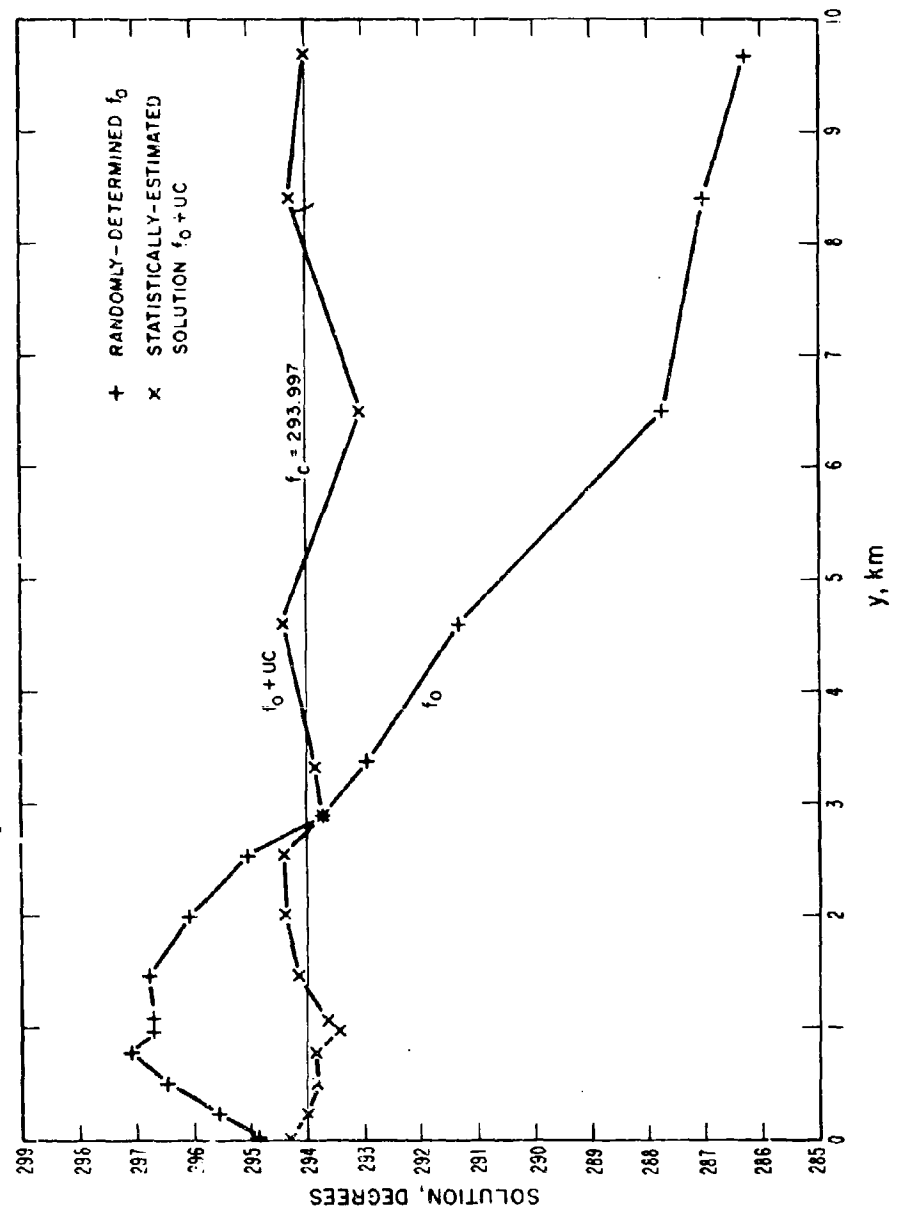
$1 \leq x_i \leq 1.98$.

Fig. 8

Solution #3 of integral equation. Sample rms solution error

$= 0.4, \; S_c = 10^{-4} \, I, \; S_f$ as in table 1, $k=5, \; n=19,$
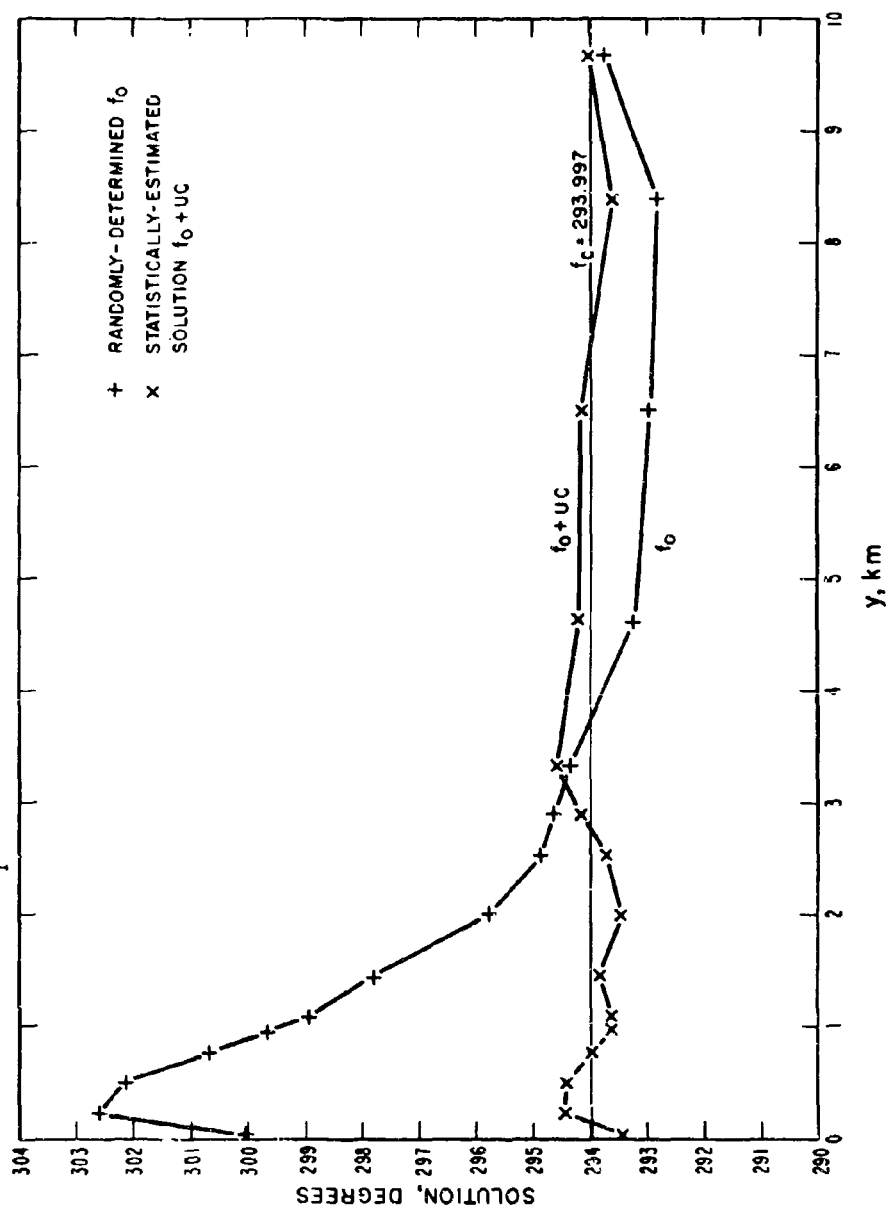
$1 \leq x_i \leq 1.98$

Fig. 9

Solution #4 of integral equation. Sample rms solution

error = 0.8, S_ϵ = 0.11, S_f as in table 1, k = 4, n=7,
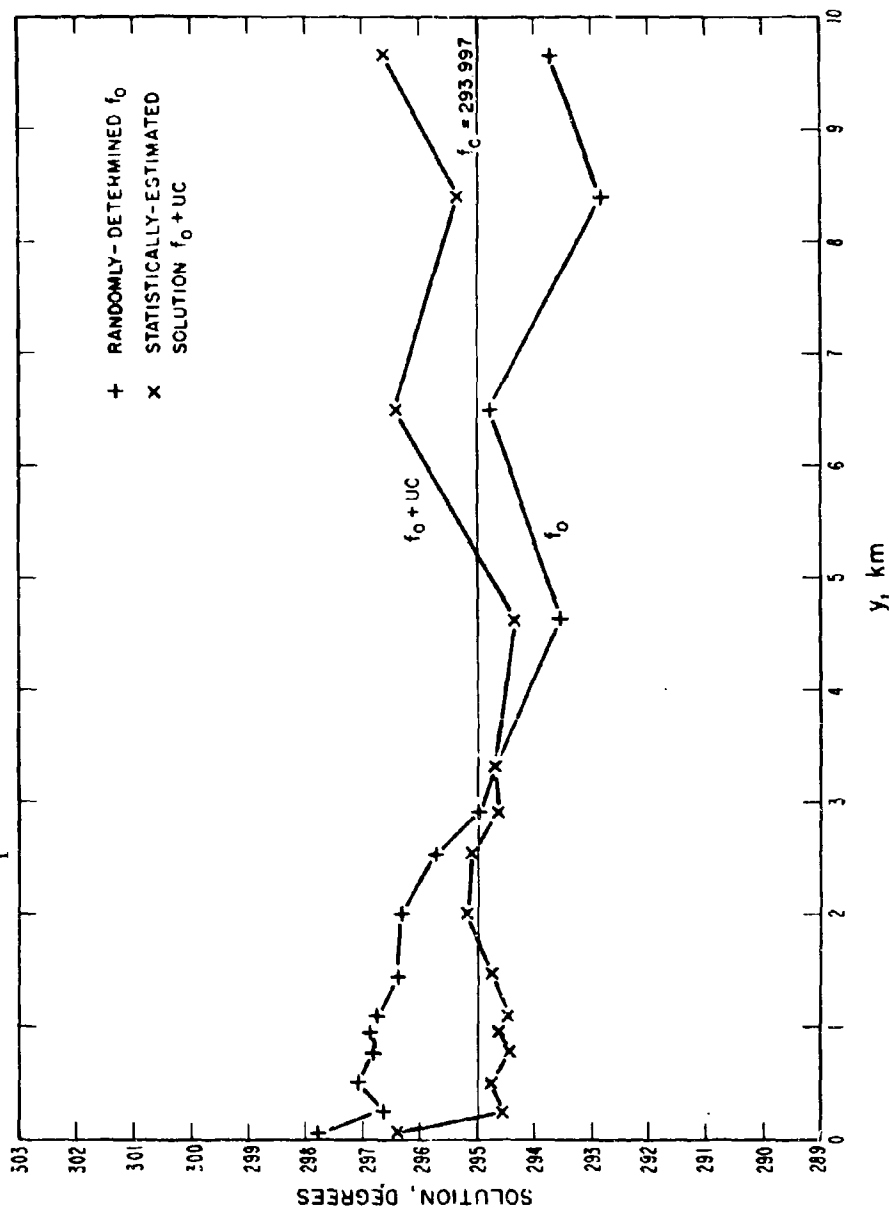
$1 \leq x_i \leq 1.98.$

Fig. 10

Solution #5 of integral equation. Sample rms solution

error = 0.8, S_ϵ = .01 I, S_f as in table 1, k = 4, n = 7,
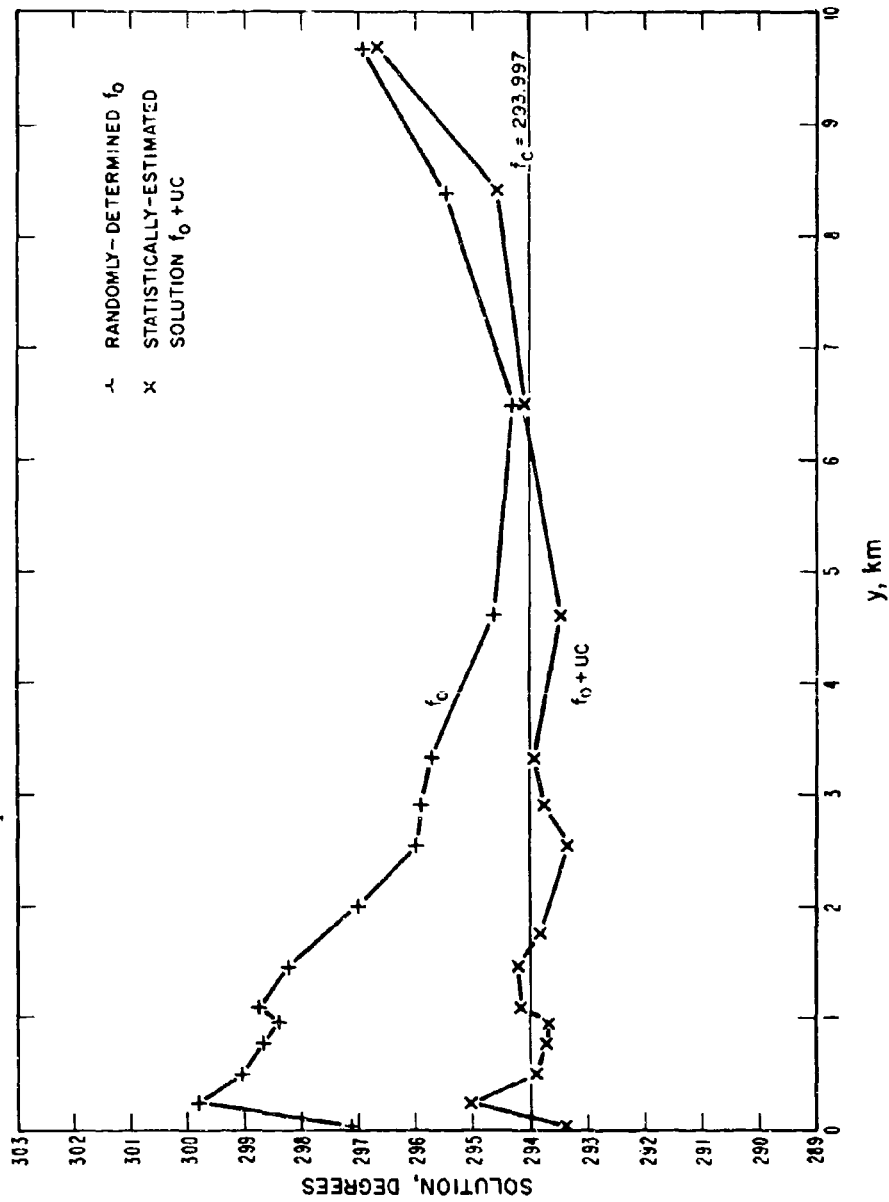
$1 \leq x_i \leq 1.98$.

Fig. 11

Solution #6 of integral equation. Sample rms solution

error = 0.9, S_e = .01 I, S_f as in table 1, k = 4, n = 7,

$1 \leq x_i \leq 1.98$.
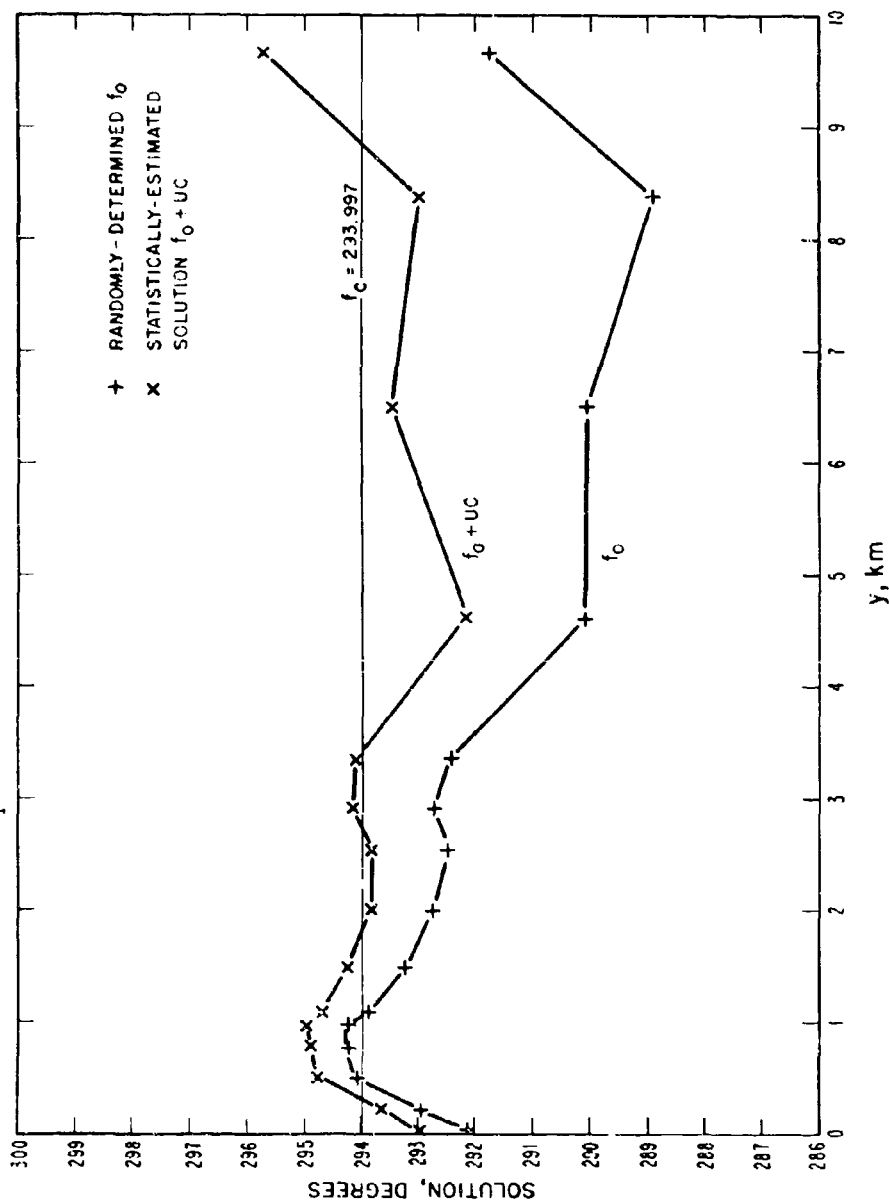
Fig. 12

Solution #7 of integral equation. Sample rms solution

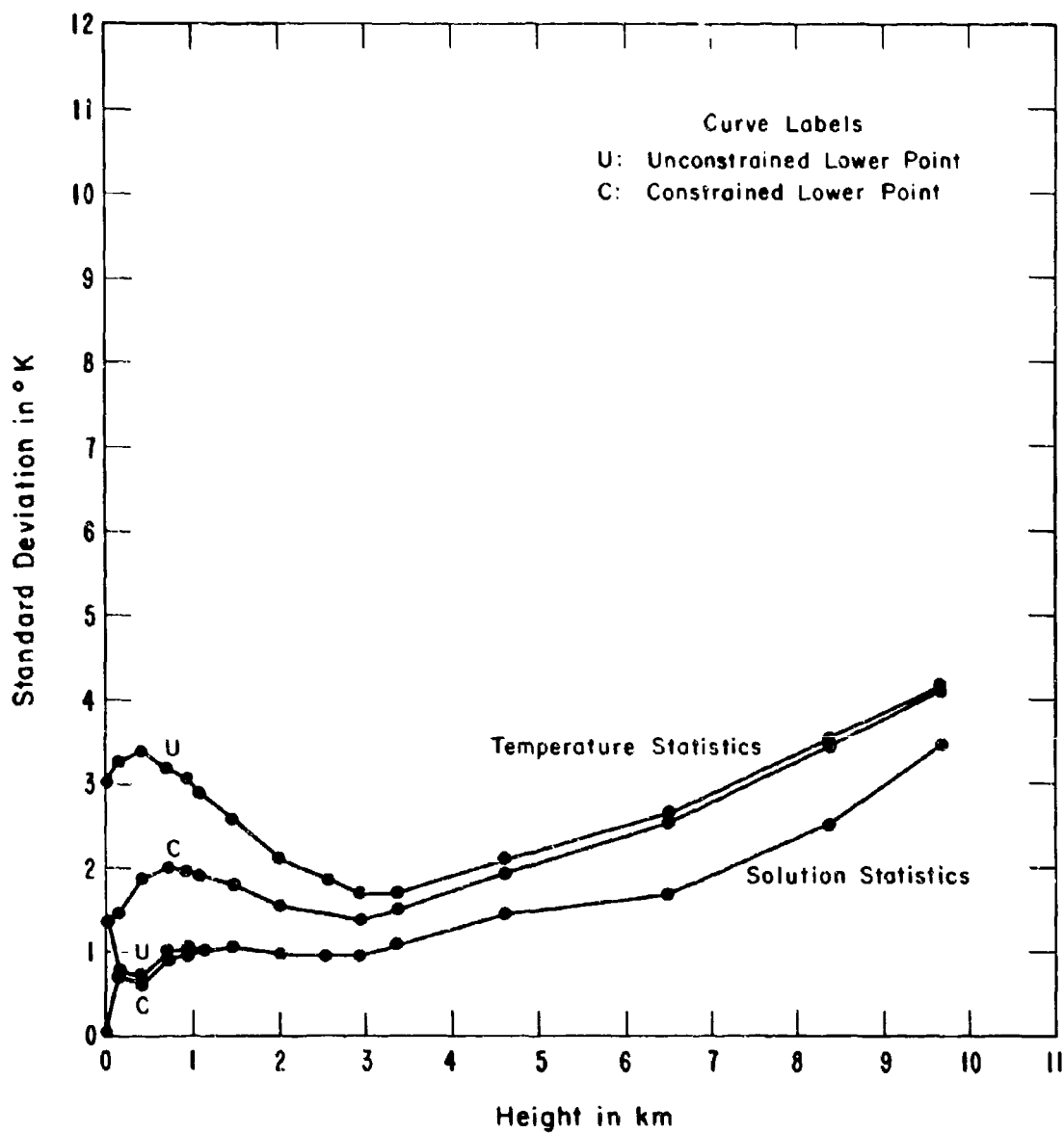error = 0.7, $S_g = .011$, S_f as in table 1, $k=4$, $n=7$,

$1 \leq x_i \leq 1.98$.
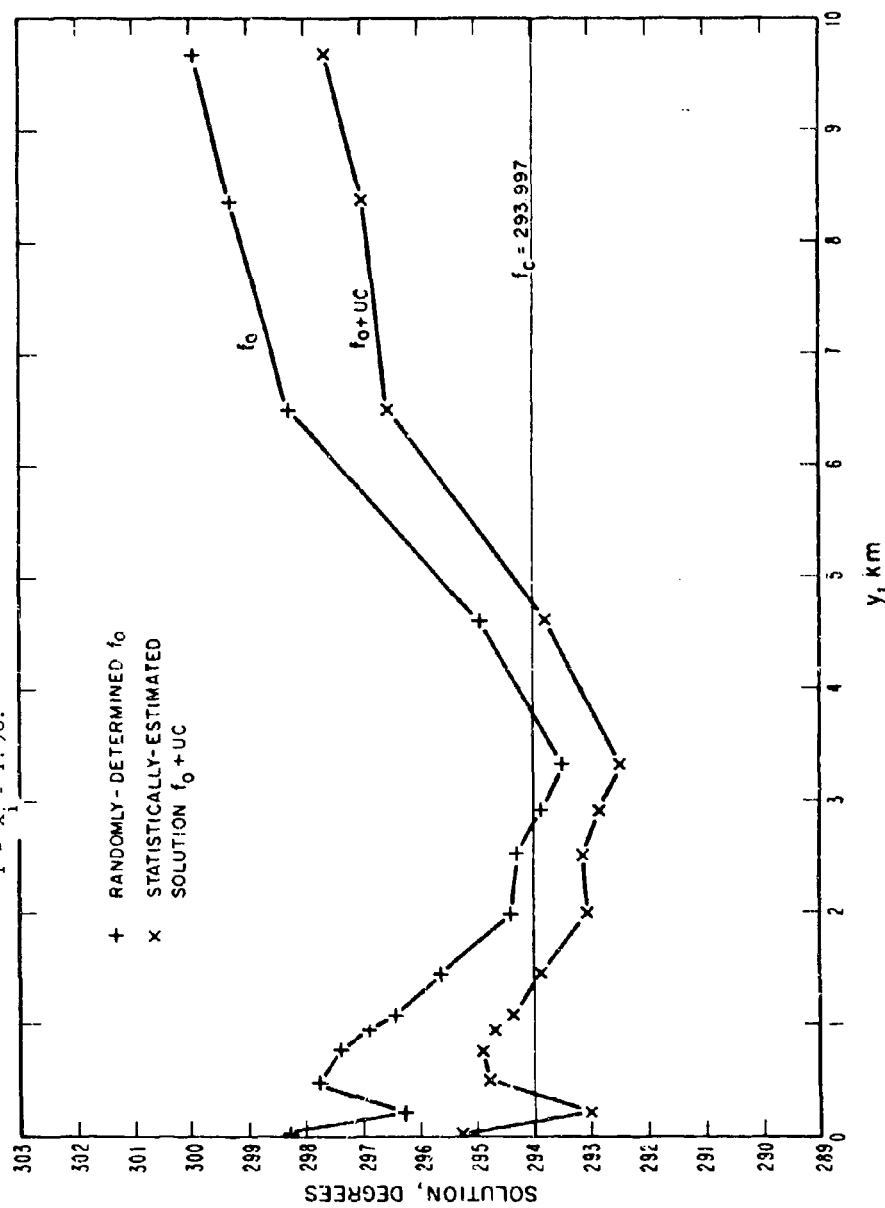
Fig. 13

Square Roots of Diagonal Elements of Covariance Matrices of Temperature Statistics, S_f, and Solution, X^{-1}, vs. Height for Denver, August, and for Measurement Errors, τ_ϵ, of .01 $^\circ$K.
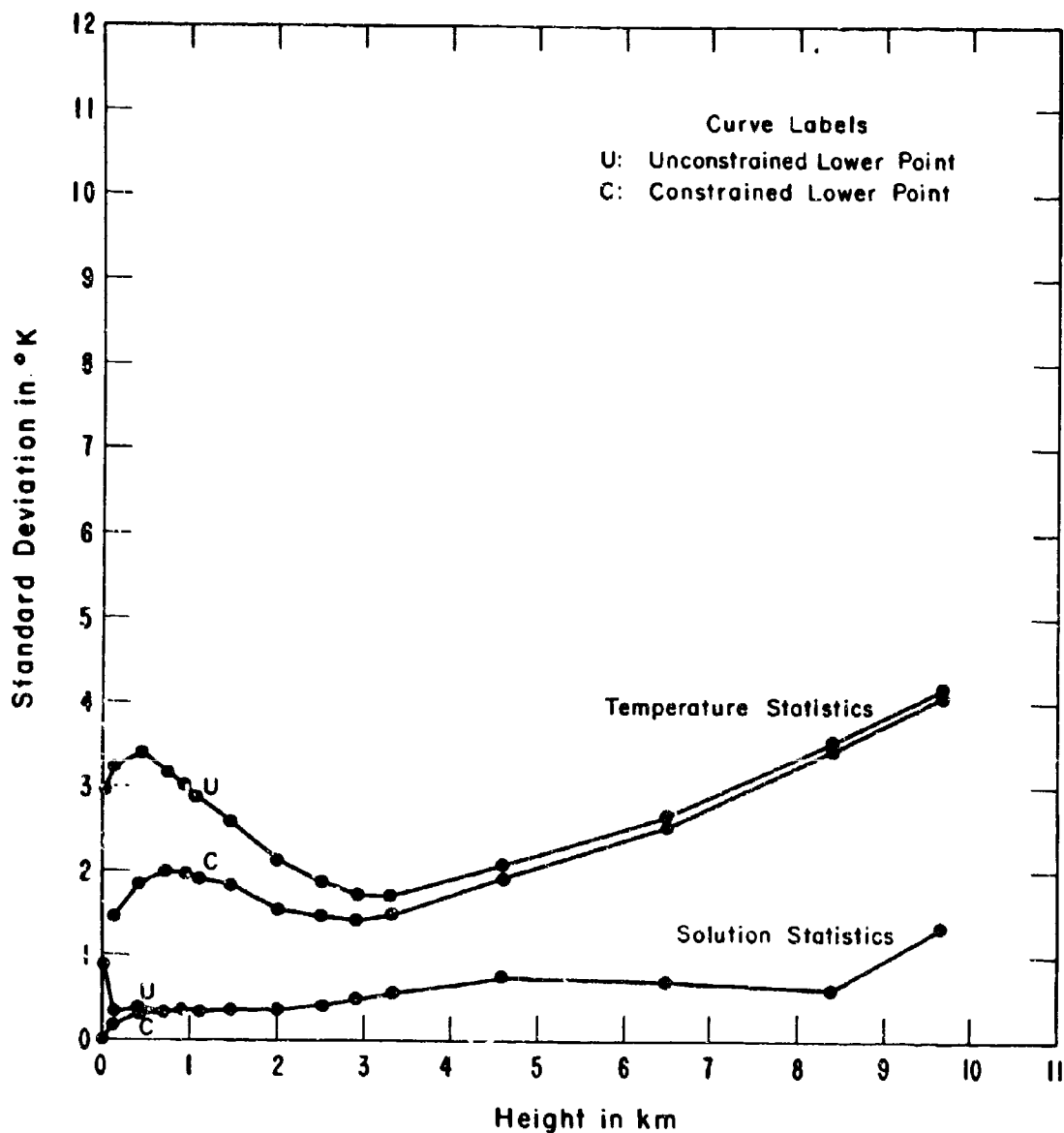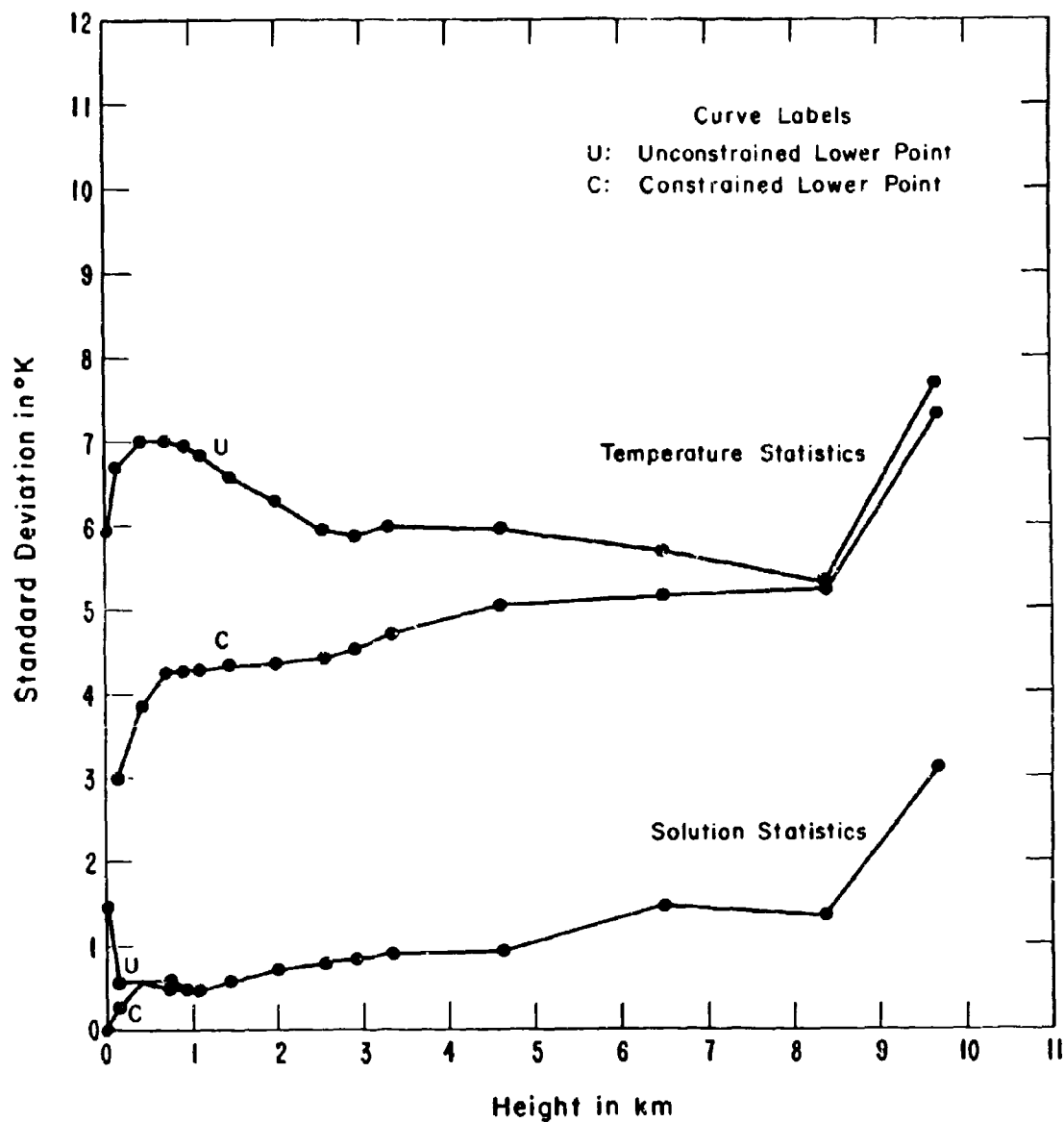

Fig. 14

Square Roots of Diagonal Elements of Covariance Matrices of Temperature Statistics, S_f, and Solution, X^{-1}_o, vs. Height for Denver, August, and for Measurement Errors, σ_ϵ, of .1 °K.
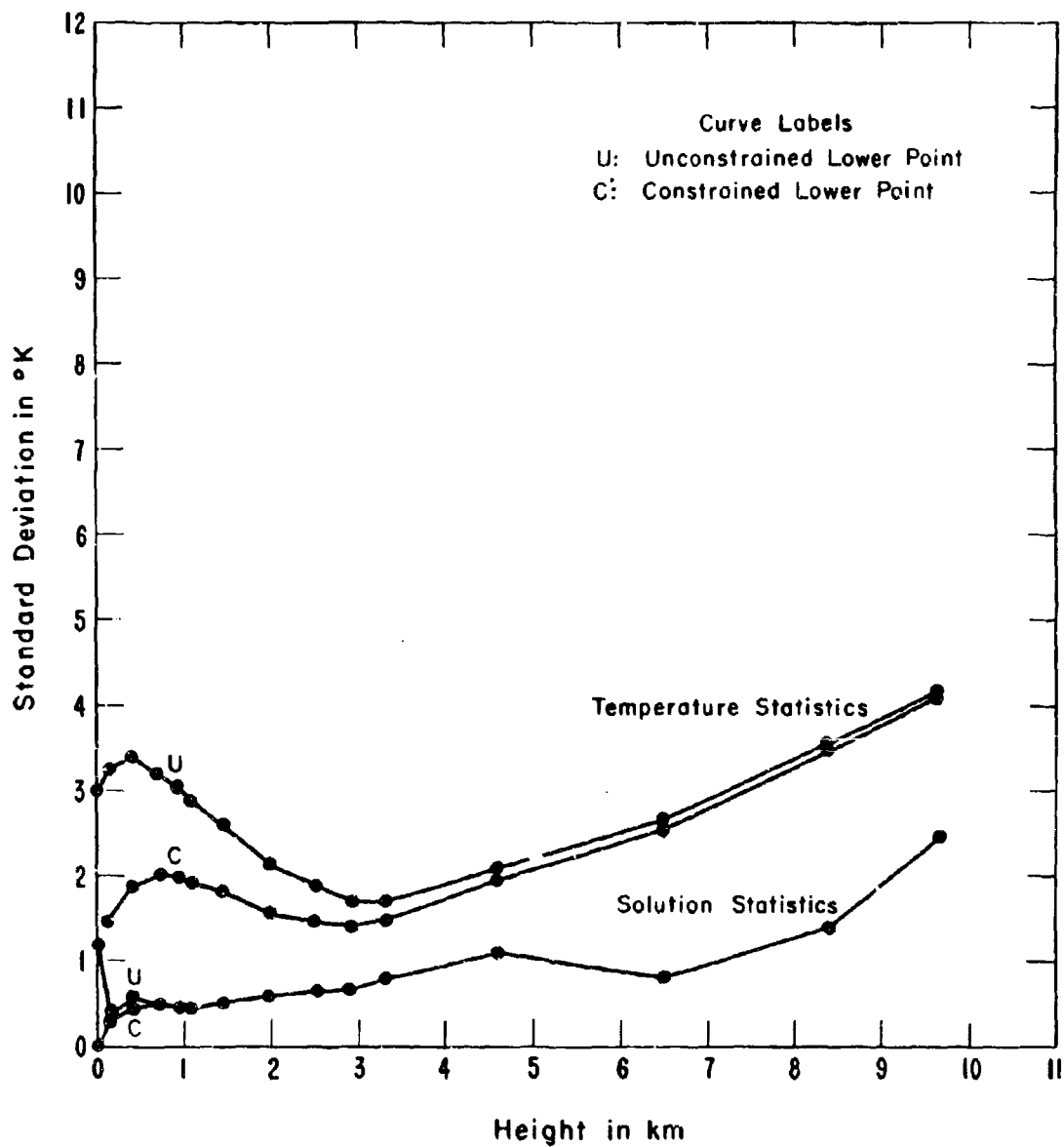
Fig. 15

Square Roots of Diagonal Elements of Covariance Matrices of Temperature Statistics, S_f, and Solution, X^{-1} vs. Height for Denver,   ust, and for Measurement Errors, σ_ϵ, of $1.0\,^\circ K$.
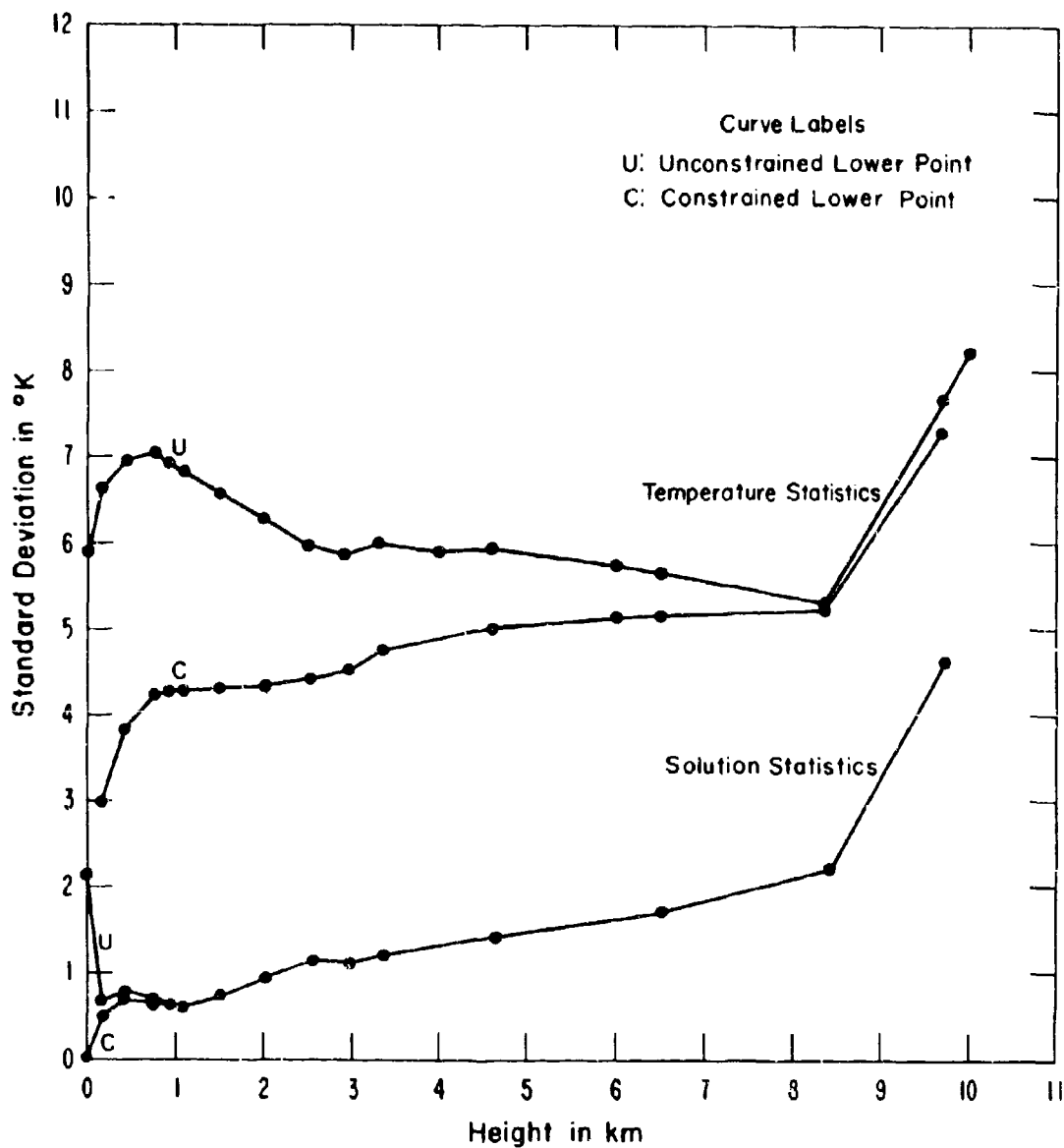

Fig. 16

Square Roots of Diagonal Elements of Covariance Matrices of Temperature Statistics, S_f, and Solution, X^{-1}, vs. Height for Denver, February, and for Measurement Errors, σ_ϵ, of .01 $^\circ K$.

Fig. 17

Square Roots of Diagonal Elements of Covariance Matrices of Temperature Statistics, S_f, and Solution, X^{-1}, vs. Height for Denver, February, and for Measurement Errors, σ_ϵ, of $.1\,^\circ K$.
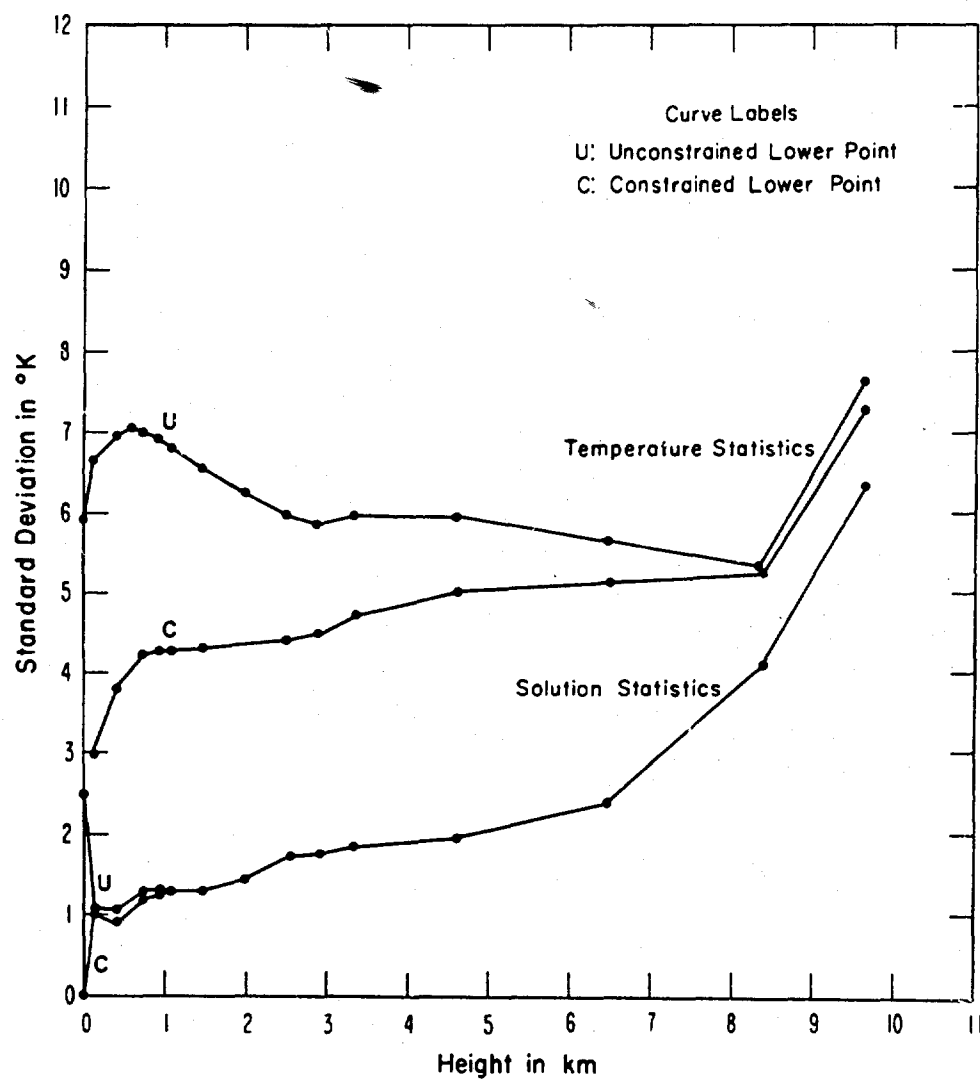

Fig. 18

Square Roots of Diagonal Elements of Covariance Matrices of Temperature Statistics, S_f, and Solution, X^{-1}, vs. Height for Denver, February, and for Measurement Errors, σ_ϵ, of 1.0 °K.

Fig. 19

Square Roots of Diagonal Elements of Covariance Matrices with Constrained Lower Point of Temperature Statistics, S_f, and Solution X^{-1}, vs. Height for Denver, August.
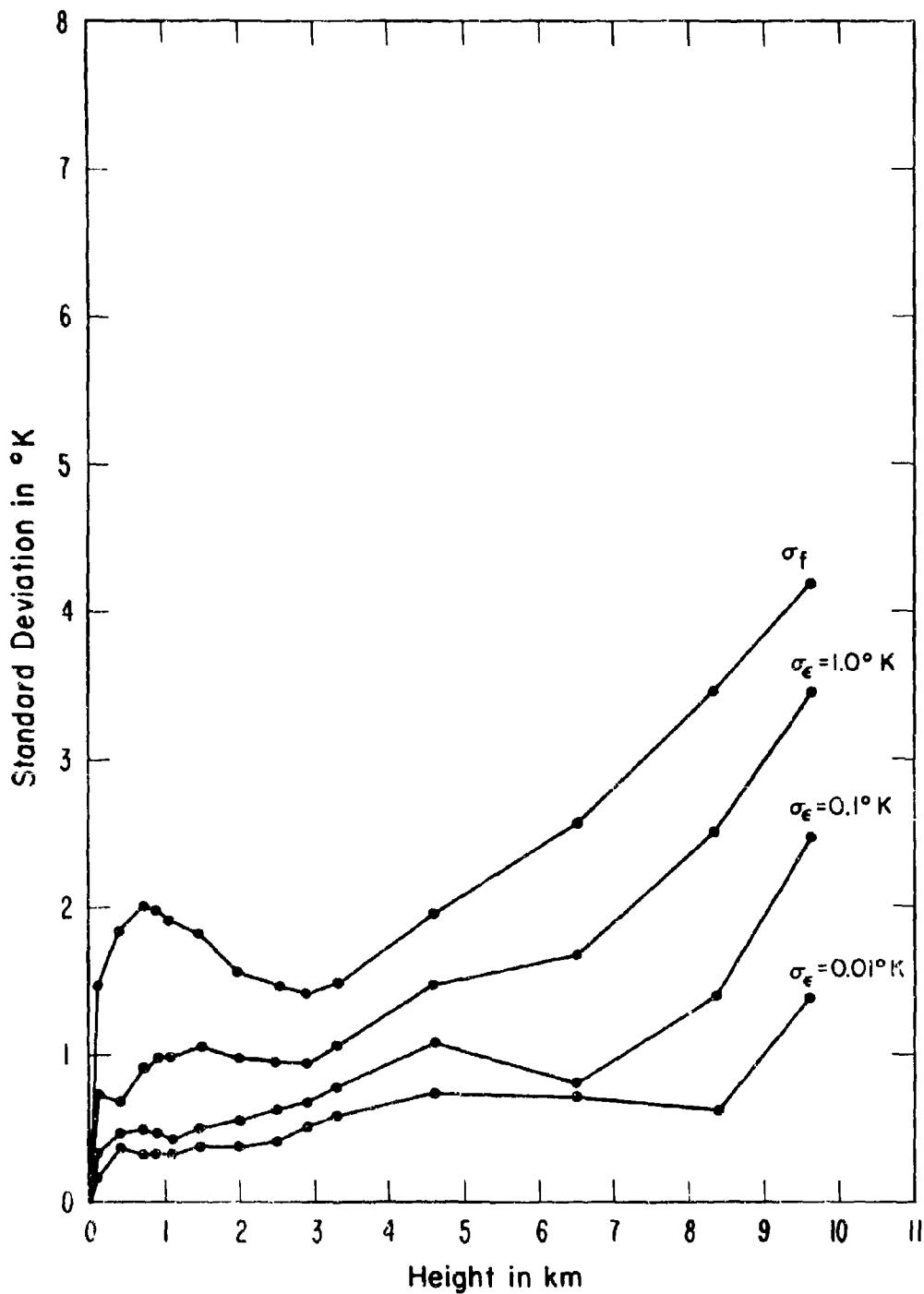
Fig. 20

Square Roots of Diagonal Elements of Covariance Matrices with Constrained Lower Point of Temperature Statistics, S_f, and Solution X^{-1}, vs. Height for Denver, February.
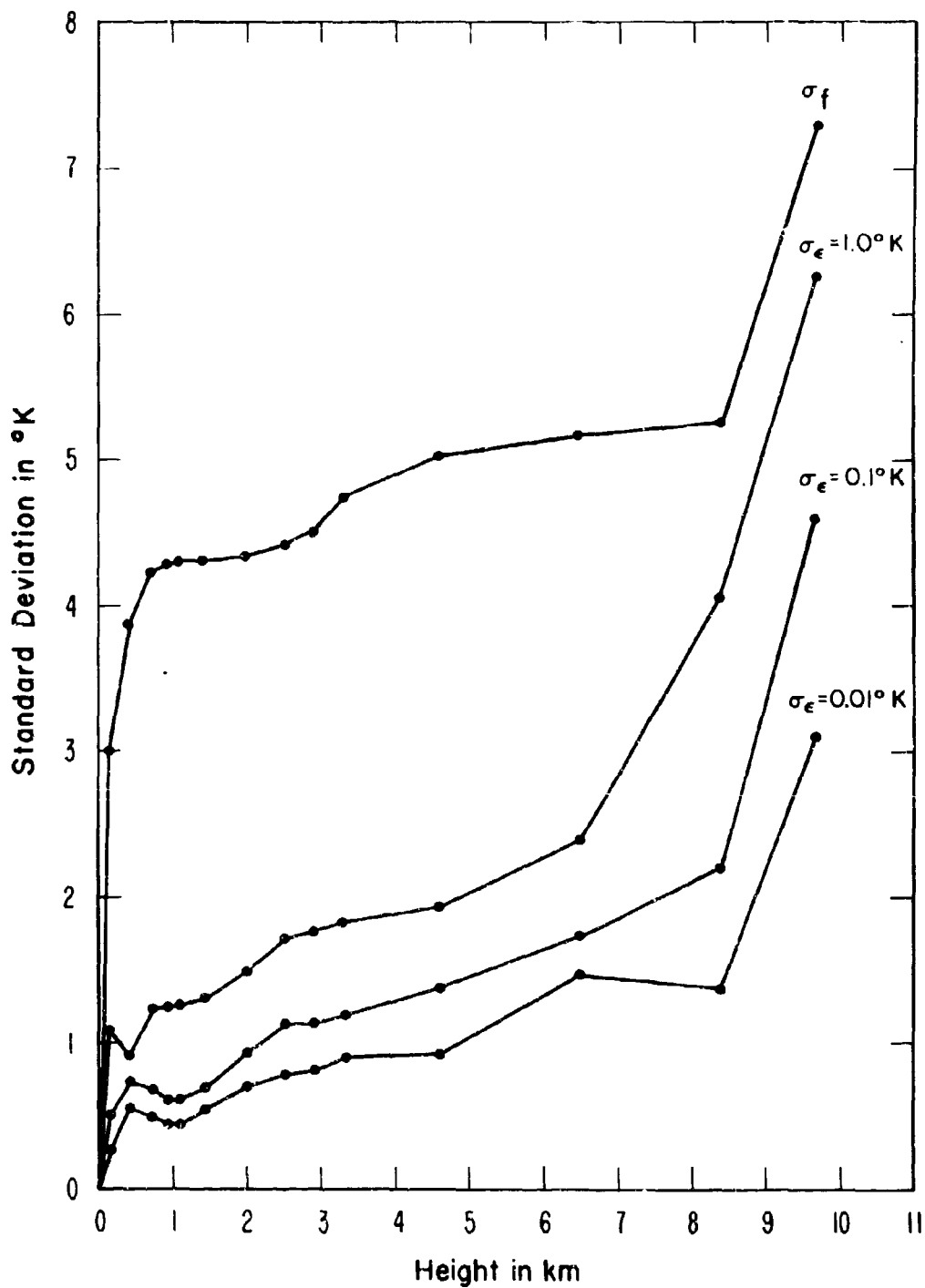
Fig. 21